Technical Note 1980-19

M. J. Tsai

Simulation Study on Detection and Estimation of Closely Spaced Optical Targets

18 March 1980

Prepared for the Department of the Army
under Electronic Systems Division Contract F19628-80-C-0002 by

Lincoln Laboratory
MASSACHUSETTS INSTITUTE OF TECHNOLOGY
LEXINGTON, MASSACHUSETTS

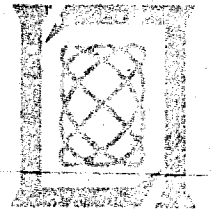

MASSACHUSETTS INSTITUTE OF TECHNOLOGY
LINCOLN LABORATORY

SIMULATION STUDY ON DETECTION AND ESTIMATION OF CLOSELY SPACED OPTICAL TARGETS

M. J. TSAI
Group 32

TECHNICAL NOTE 1980-19

18 MARCH 1980

LEXINGTON MASSACHUSETTS

ABSTRACT

In this report the detection and estimation of closely spaced optical targets are studied using simulation. The observed signal which originates from two point targets may exhibit only one apparent peak when they are located within one detector width. The Akaike information criterion and a maximum likelihood estimator are used to detect and estimate such unresolved targets. For target separation between 3/4 and 1 detector width the detection rate is high, the estimator is unbiased and the estimation variance is close to the Cramer-Rao bound. The performance degrades greatly when the separation becomes smaller. This loss in performance is attributed to the increasing interference between the two targets and the difficulty in providing a "good" initial guess for the estimator.

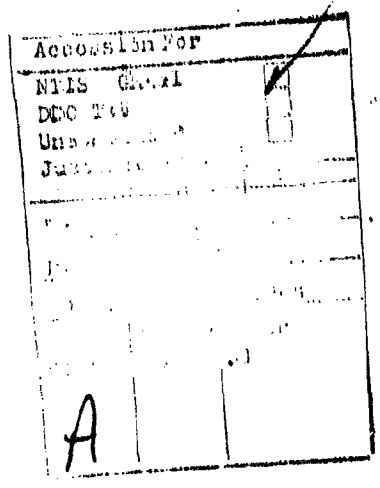

CONTENTS

I. INTRODUCTION

In the hierarchy of BMD (Ballistic Missile Defense) systems functions, closely spaced object (CSO) resolution occurs early in the sequence of events and consequently influences the performance of the subsequent functions to different degrees. It is very important to assess the CSO resolution capability of the sensor systems employed in every BMD system study before one can determine the overall BMD system performance. The CSO resolution capability is clearly dependent upon the sensor system and the threat characteristics considered in the BMD system study. Current attention has been focused on a variety of passive optical sensor systems employed in the Layered Defense System against threats at long ranges with high angular density. Several studies have been completed recently in assessing the CSO resolution performance for various optical systems [1-4]. The CSO parameter estimation performance can either be predicted by theoretical lower bounds, say the Cramer-Rao lower bounds [1-4], or be evaluated by the Monte-Carlo simulation of specific algorithms. In the earlier studies [1-4], the estimation accuracy for the intensity and position of the CSO's were presented for various lens apertures and noise models under the assumption that the exact number of targets present is known. The CSO detection performance was not presented in these studies.

It is the purpose of this report to address the following

issues through a simulation study: Is the above-mentioned theoretical lower bound achievable in practice? Can the number of targets present in the CSO cluster be determined with certainty so that the assumption made is true? In the simulation, a maximum likelihood estimator is implemented for the CSO parameter estimation and the Akaike information criterion (AIC) is employed to determine the number of targets. A specific sensor and noise model as well as the detector scanning mode is selected for this study. For other sensors and noise models and detector patterns, a similar CSO detection and estimation algorithm can be implemented very easily. This work is in its initial stages. The findings reported here are interesting but not necessarily complete and conclusive. Further investigations are currently in progress and will be reported in future reports.

The problems concerned in this study are first stated in section 2. The models of signal and noise in a single scanning detector environment are outlined in this section. The methods for detection and estimation are described in section 3. Section 4 presents the Monte-Carlo simulation results of detection and estimation performance. The estimation performance thus obtained is also compared with the theoretical result. Some details of the computational aspects of the algorithm and the program listing are attached in the appendices.

II. PROBLEM STATEMENT

For the purpose of this simulation study, the optical sensor system can be simplified and is represented in Fig. 1. The optical point targets which are in the field-of-view of the sensor will form an image on the focal plane. This image is often referred to as the point spread function (PSF). An optical detector is usually employed to scan the image in a fixed direction. The spatial structure of the optical image is thus converted into a temporal electrical signal. This signal is then subject to amplification, filtering and analog-to-digital conversion before entering the signal processor. Noise sources which can be introduced at various points of the system include the background radiation noise, scanning noise, optical-electrical conversion noise, amplifier noise and quantization noise. For simplicity, it is assumed in this study that these noise sources can be lumped together and represented by an additive white gaussian noise (WGN), n(t). The observations available to the detection and estimation processor can then be written as

$$y(t_\ell) = s_d(t_\ell) + n(t_\ell) \qquad \ell=1, 2,\ldots,k \tag{1}$$

where $s_d(t)$ is the desired signal. Given these observations the processor is then required to perform the following two functions:

1. Determine how many targets are embedded in the

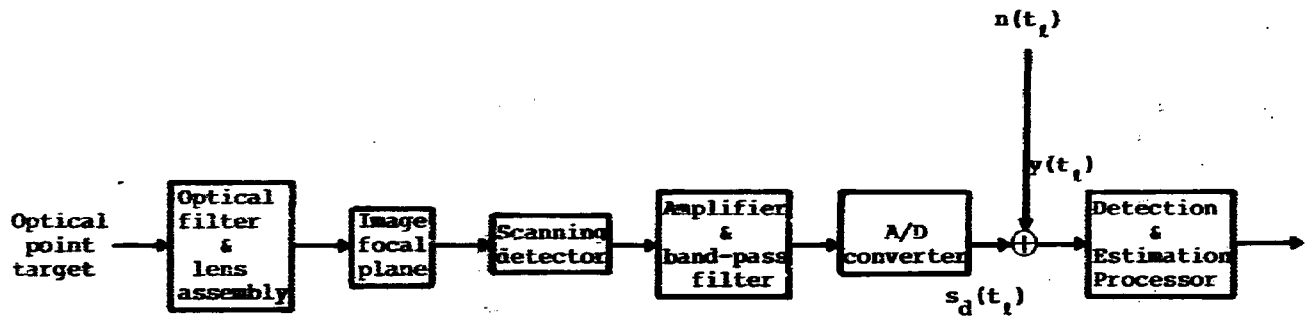

Fig. 1. Optical detection/estimation system.

observed signal (detection problem)

2. Obtain intensities and positions of the targets (estimation problem)

It is the purpose of this report to describe an algorithm for such a processor and to evaluate its performance.

Suppose that there are n point targets which lie along the scanning direction of the detector.* The desired signal $s_d(t)$ is simply given by

$$s_d(t) = \sum_{i=1}^{n} a_i s_o(t-\tau_i) \tag{2}$$

where a_i and τ_i are the intensity and position of the i^{th} target; $s_o(t)$ is the basic target response generated by a target of unit intensity lying on the optical axis. The shape of $s_o(t)$ depends upon the PSF of the particular aperture and the scanning response function of the detector. Suppose the aperture is annular with 50% obscuration; the detector response function is uniform and equal to unity within a rectangular gate and equal to zero elsewhere. Then $s_o(t)$ is given by [6].

$$s_o(t) = \int_{-\beta_y/2}^{\beta_y/2} \int_{\alpha t-\beta_x/2}^{\alpha t+\beta_x/2} s_f(x,y)\,dx\,dy \tag{3a}$$

*This assumption has to be made because the cross-scan position of a target can not be resolved by a single detector.

where

$$s_f(x,y) = \left\{ \frac{8}{3} \frac{J_1[\pi(x^2+y^2)^{\frac{1}{2}}]}{\pi(x^2+y^2)^{\frac{1}{2}}} - \frac{4}{3} \frac{J_1[\frac{\pi}{2}(x^2+y^2)^{\frac{1}{2}}]}{\pi(x^2+y^2)^{\frac{1}{2}}} \right\}^2 . \qquad (3b)$$

Here, $J_1(\cdot)$ is the Bessel function of first kind; α is the angular scanning rate normalized by the optical diffraction limit λ/d; β_x and β_y are the in-scan and cross-scan angular dimensions of the detector normalized by λ/d. Without loss of generality, the scanning rate can be assumed equal to 1 and thus the time variable t is equivalent to the angular variable θ. These two variables will be used interchangeably throughout this report.

The basic optical pulse, $s_o(t)$, is depicted in Fig. 2 for a detector with $\beta_x=2$ and $\beta_y=6$. Note that there is a slight overshoot near the center of the pulse. Fig. 3 illustrates several sample waveforms, y(t), from detectors of identical size for the case of 2 CSO's with various intensities* and positions. The variance of the WGN is equal to 1. It can be seen that the 2 targets which are separated by 2.5 λ/d (Fig. 3a) correspond to two-peaks of y(t). In this case they can be detected and estimated with a matched filter followed by a peak detector. However, in Figs. 3(b) - 3(d), the two targets which are located within one detector width($2\lambda/d$) interfere with each other to such a degree that only one apparent

*The signal $s_d(t) = as_o(t)$ has the peak at the center (t=0) equal to 10 for a = 9.08.

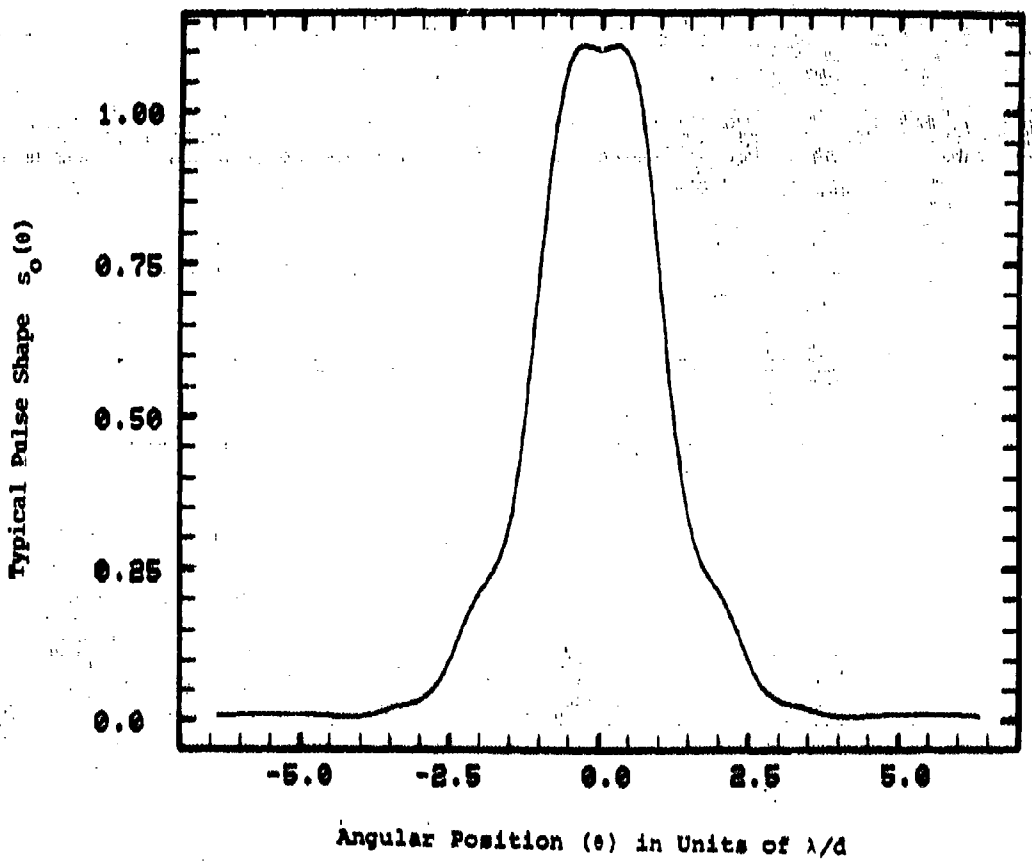

Fig. 2. Typical pulse shape, Eq.(3).

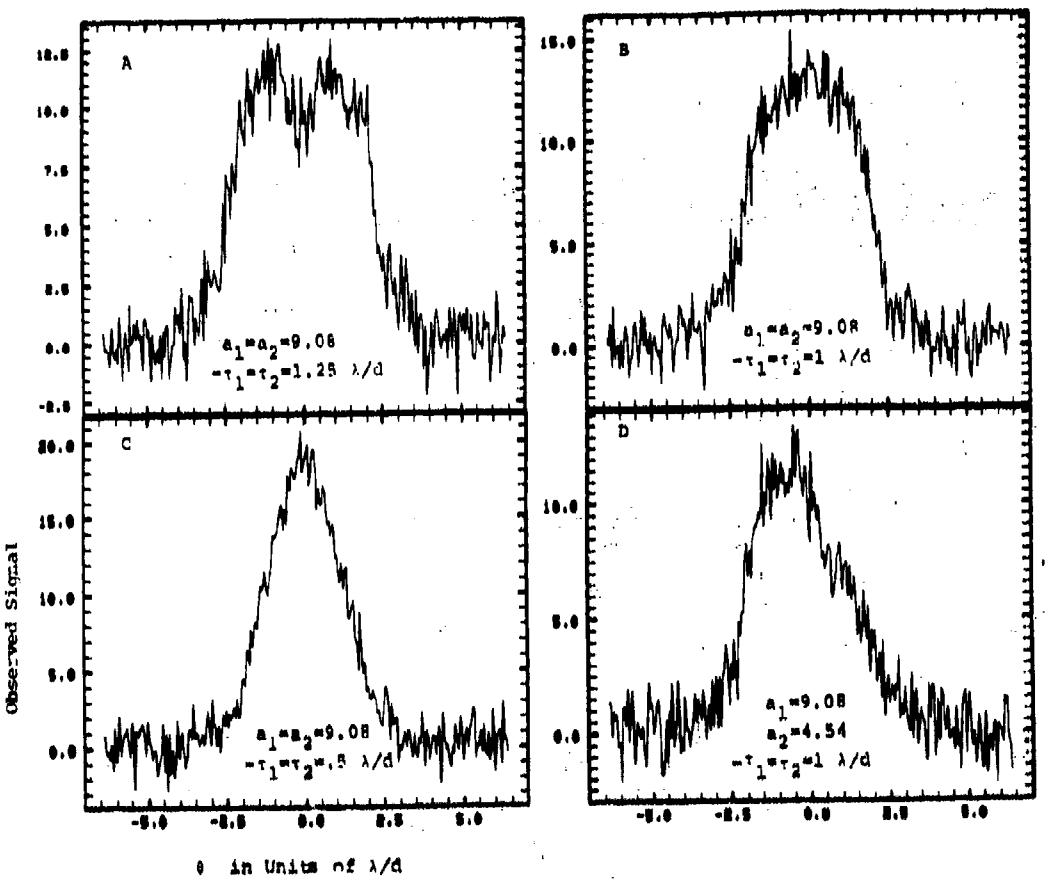

Fig. 3(a-d). Some examples of the observed signal, y(t), in the case of two CSO's; the variance of the WGN is equal to 1.

peak is observed in the resulting noisy waveform. A simple peak detector may not be capable of resolving satisfactorily the two targets in these examples. Other more sophisticated detection/ estimation schemes are required for this purpose.

III. METHODS

3.1 Akaike Information Criterion

One approach for determining the number of targets imbedded in the observed data is to apply the generalized likelihood ratio (GLR) test. There are some difficulties in applying this method. First, the distribution of the GLR is hard to find so that the behavior of the test may not be known exactly. Second, since the test can only be applied to two classes at one time, multiple application of the test is required for the present problem. Third, the choice of the test threshold is usually very subjective.

Akaike has advocated a new approach, termed the Akaike information criterion (AIC), for determining the order of the correct model (for the problem here, the order is the number of targets present) [5]. This information criterion is based on an extension of the maximum likelihood principle starting from the fundamental notation of entropy in statistical mechanics and the Kullback-Leibler information quantity. The final statistic used to optimally choose the order is defined by

$$\text{AIC} = (-2)\ \log_e(\text{maximum likelihood}) + 2(\text{number of free parameters}) \tag{4}$$

The correct model is that which minimizes this criterion.

Note that the first term in the definition of the AIC represents a penalty of "poor fit" and the second term characterizes increased unreliability. This second term is essential because the maximum value of the likelihood function with the higher order model (model with more parameters) is usually greater than that of the smaller model and therefore without this term, the model with higher order would be favored. Qualitatively speaking, the AIC provides a mathematical formulation of the principle of parsimony in model building.

The AIC has found many applications in various fields, particularly in the autoregressive model fitting of time-series analysis. Since the theory is general, it is easily applied to the detection problem stated in the last section. Two obvious advantages for using the AIC in this problem can be seen from Eq. (4):

1. The AIC is easy to apply; Eq. (4) is very simple.
2. The AIC combines the detection problem with the estimation problem. For detection (determining the order of the model) the information from estimation (finding the maximum likelihood function) is needed. Once the detection is done, the maximum likelihood estimates of parameters in the correct model are also available without additional effort.

Although the AIC is derived from the ideas of information

theory, there seems to be no particular basis for the penalty factor 2. Some investigators, applying the AIC in their particular problems, reported that this factor should be between 3.5 and 4 [7]. It can be shown that the AIC decision rule is equivalent to the hypothesis testing procedure at an appropriate significance level in the case of two classes. Using different values for the penalty factor is analogous to adjusting the significance level. The effect of this factor will be reported in this study. For this purpose, the AIC can be rewritten as

$$AIC(i) = (-2)\log_e(\text{maximum likelihood}) + \eta(2i) \qquad (5)$$

where η is the penalty factor and i is the number of targets present.*

It is reasonable to assume that AIC(i) is a discrete unimodal function of i for a fixed value of η. Therefore the detection procedure is simply as follows:

Step 1: Start with i=0; compute AIC = AIC(0).

Step 2: Increment i by 1.

Step 3: Compute AIC(i).

Step 4: If AIC(i) is greater than AIC, go to Step 5. Otherwise, set AIC = AIC(i) and go back to Step 2.

*Two parameters, intensity and position, are associated with each target.

Step 5: Stop; the number of targets present is equal to (i-1).

3.2 Maximum Likelihood Estimator

The maximum likelihood estimator (MLE) is implied in the AIC procedure. This estimator posesses several nice properties. It can be shown that the MLE, under rather general conditions, is asymptotically unbiased and efficient; it yields the same results as the least-square method for the case of additive white gaussian noise.

For the signal model described in section 2, the likelihood function can be written as

$$\ell(\underline{x},\sigma) = \frac{1}{(2\pi)^{k/2}\,\sigma^{k}} \exp\left(-\frac{1}{2\sigma^2}(\underline{y}-\Omega_n\underline{a})^T(\underline{y}-\Omega_n\underline{a})\right) \tag{6}$$

where

$$\Omega_n = \begin{pmatrix} s_o(t_1-\tau_1) & \cdots & s_o(t_1-\tau_n) \\ \vdots & & \vdots \\ s_o(t_k-\tau_1) & \cdots & s_o(t_k-\tau_n) \end{pmatrix} \tag{7}$$

$$\underline{Y} = (y(t_1),\ y(t_2),\ldots,y(t_k))^T$$

$$\underline{x} = \begin{pmatrix} \underline{a} \\ \underline{\tau} \end{pmatrix} = (a_1,..,a_n,\ \tau_1,..,\tau_n)^T = (x_1,..,x_n,\ x_{n+1},..,x_{2n})^T$$

and σ, considered as an unknown parameter, is the standard deviation of the WGN. The maximum likelihood estimates of $\underline{x}$ and σ, denoted by $\hat{\underline{x}} = \begin{pmatrix} \hat{\underline{a}} \\ \hat{\tau} \end{pmatrix}$ and $\hat{\sigma}$ are the values of $\underline{x}$ and σ which maximize $\ell(\underline{x},\sigma)$. Since the logarithm is a strictly increasing function, the maximization of $\ell(\underline{x},\sigma)$ and $\log_e \ell(\underline{x},\sigma)$ are equivalent. Let

$$J(\underline{x},\sigma) = \log_e \ell(\underline{x},\sigma) =$$

$$= -\frac{k}{2}\log_e(2\pi) - k\log_e\sigma - \frac{1}{2\sigma^2}(\underline{y}-Q_n\underline{a})^T(\underline{y}-Q_n\underline{a}) \qquad (8)$$

The maximum value of this function is the first term needed to evaluate the AIC.

It is usually not necessary to estimate the unknown σ explicitly and it can be dropped from the expression for J. By taking the derivative of J with respect to σ and setting it to zero, $\hat{\sigma}$ is obtained as

$$\hat{\sigma} = \left(\frac{1}{k}(\underline{y}-Q_n\underline{a})^T(\underline{y}-Q_n\underline{a})\right)^{\frac{1}{2}} \qquad (9)$$

By replacing σ with $\hat{\sigma}$, Eq. (8) becomes

$$J(\underline{x}) = -\frac{k}{2}\left\{\log_e(2\pi) + 1 + \log_e\left(\frac{1}{k}(\underline{y}-Q_n\underline{a})^T(\underline{y}-Q_n\underline{a})\right)\right\} \qquad (10)$$

Using this logarithmic likelihood function with the first two nuisance terms discarded, the AIC given by Eq. (5) can be

written as

$$AIC(i) = k\log_e \hat{\sigma}^2 + 2ni. \tag{11}$$

It is clear that as far as the maximization is concerned $J(\underline{x})$ in Eq. (10) can be replaced with

$$J(\underline{x}) = -(\underline{y}-Q_n\underline{a})^T(\underline{y}-Q_n\underline{a}). \tag{12}$$

By setting the gradient of $J(\underline{x})$ with respect to $\underline{a}$ equal to zero, the intenstiy estimate, $\hat{\underline{a}}$, can be obtained as

$$\hat{\underline{a}} = (Q_n{}^T Q_n)^{-1} Q_n{}^T \underline{y} . \tag{13}$$

Substituting $\hat{\underline{a}}$ in Eq. (12), J can be rewritten as

$$J(\underline{x}) = \underline{y}^T\left[Q_n(Q_n{}^T Q_n)^{-1} Q_n{}^T - I\right]\underline{y} . \tag{14}$$

The maximization of the likelihood function can be done with respect to expressions given by either Eq. (12) or Eq. (14). The former involves 2n parameters and the latter involves only n parameters but requries ratrix compuations which usually need more computer time. Experience seems to indicate that it is easier to use Eq. (12).

It should be noted that the J function is nonlinear on the unknown parameters. Its maximization is implemented here be using the Quasi-Newton method [8] which is an iteration procedure starting with an initial guess. This method is appealing because it possesses the quadratic convergence property near the maximum of the criterion function (like the Newton method) and avoids the difficulty involved in computing the inverse of the Hessian matrix at each iteration (unlike the Newton method). At each iteration, the gradient, $\nabla J(\underline{x}) = \{\frac{\partial J(\underline{x})}{\partial x_i}, i=1,\ldots,2n\}$, is required, which, from Eq. (12), is given by

$$\frac{\partial J(\underline{x})}{\partial x_i} = \sum_{\ell=1}^{k} (y(t_\ell) - s_d(t_\ell)) \frac{\partial s_d(t_\ell)}{\partial x_i} . \tag{15}$$

Here, from Eq. (2),

$$\frac{\partial s_d(t)}{\partial x_i} = \begin{cases} s_o(t-\tau_i) & x_i=a_i \\ -a_i \dot{s}_o(t-\tau_i) & x_i=\tau_i \end{cases} \tag{16}$$

and, from Eq. (3),

$$\dot{s}_o(t) = \alpha \int_{-\beta_y/2}^{\beta_y/2} \left[s_f(\alpha t+\beta_x/2, y) - s_f(\alpha t-\beta_x/2, y) \right] dy. \tag{17}$$

The unknown parameters are not entirely free but subject to two types of constraints. The intensity of any target, a_i, is physically constrained to be non-negative. This constraints can

be released by substituting b_i^2 for a_i. By doing so, nothing is changed except that the parameter set becomes $\underline{x} = \{b_1,\ldots,b_n, \tau_1,\ldots,\tau_n\}^T$ and Eq. (16) is replaced by

$$\frac{\partial s_d(t)}{\partial x_i} = \begin{cases} 2b_i s_o(t-\tau_i) & x_i=b_i \\ -b_i^2 \dfrac{\partial s_o(t-\tau_i)}{\partial t} & x_i=\tau_i. \end{cases} \tag{18}$$

The final estimate $\hat{a}_i$ can be obtained by setting $\hat{a}_i = \hat{b}_i^2$. Suppose now the sequence of observations, $\underline{y}$, is obtained in the range from $\theta_o-\gamma/2$ to $\theta_o+\gamma/2$ where γ is the angular distance covered by the observations and θ_o is the central point of the range. In practice, it can be assumed that the admissible range for τ_i, center of the i^{th} target response, is also within this range. In other words, only targets with center falling in this range will be idenfified. This additional range constraint will be incorporated into the Quasi-Newton method.

The choice of initial guess is a crucial step for the Quasi-Newton method. A good initial guess can lead the iteration process to converging to the correct maximum in a relatively small number of iterations. On the other hand, for a bad initial guess, the iteration process might converge to a local maximum, oscillate around the maximum or not converge at all.

One method for generating the initial guess is the pure ran-

dom search. This method consists of computing $J(\underline{I})^*$ at N random points drawn from a probability distribution uniform over the entire parameter space and selecting the point with the greatest value of $J(\underline{I})$ as the initial guess. If it is assumed that each parameter can vary between 0 and 100% and that the optimal parameter set which correspond to the global maximum of $J(\underline{I})$ is to be located within 10% of each parameter then the probability of locating the optimum in N trials is [9]

$$p = 1-(1-10^{-n})^{N} . \tag{19}$$

Conversely the number of trials required to have a 90% probability of locating the optimum is

$$N = 1/\log\left(\frac{1}{1-10^{-n}}\right) \approx 2.3\times 10^{n}. \tag{20}$$

Obviously, the required number of trials increases rapidly with the number of unknown parameters, n. If there exists a single target (n=1) the pure random search seems able to yield a "good" initial guess within a reasonable computation time. However for more than one target this method becomes impractical.

A more practical approach is to use the pure random search in conjunction with a priori knowledge. As pointed out earlier,

*For the purpose of selecting an initial guess, Eq. (14) instead of Eq. (12) is used.

in applying the AIC procedure to determine the number of targets, the statistics AIC(i), i=1, 2,..., are computed in ascending sequence. At each step the likelihood function is maximized iteratively starting with an initial guess. It seems feasible to select the initial guess of the $(i+1)^{th}$ step in such a way that the initial values of the first i parameters are equal to the i estimates from the previous step and the initial value of the remaining parameter is chosen from pure random search. Thus, the initial guess for any model (number of target) is obtained by performing a one-parameter search which is easier numerically. This approach guarantees that the maximum likelihood function of the $(i+1)^{th}$ step is no less than that at the i^{th} step. However, if, for the model of i+1 targets, the first i components of the true optimum in the i+1 parameter space are far from the optimal point determined in step i, the initial guess obtained in this way is usually not "good" for the $(i+1)^{th}$ step. The actual implementation of this approach is described in the appendices.

IV. SIMULATION RESULTS AND DISCUSSIONS

The performance of detecting the number of targets present and estimating the parameters of these targets is evaluated by Monte-Carlo simulation. The simulation algorithm has been described in the previous section and more details are given in the appendices. In presenting the results, some system parameters must be specified. It is assumed that the signal available to the processor is observed in an angular range of $\pm$ 6.3 λ/d from the center of the focal plane. The signal is sampled uniformly in this range at an interval of .2 λ/d. The total number of observations is 64. The signal is the product of an annular aperture with 50% obscuration and a scanning photo-detector with in-scan and cross-scan dimensions equal to 2 λ/d^* and 6 λ/d respectively. The number of Monte-Carlo runs is fixed at 100 for every case discussed in the following.

4.1 Detection Performance

First consider the case where at most one target may exist. One must decide between two hypotheses; H_o: no-target and H_1: one-target present. For this case it is only necessary to compute AIC(0) and AIC(1), and the decision rule accepts H_o(H_1) if AIC(0) (AIC(1)) is the smaller of the two. The detection performance

*The in-scan dimension of the detector is approximately equal to the diameter of the blur size (diameter of the first dark ring) of the PSF.

curve (false alarm rate vs. leakage rate) is shown in Fig. 4. The false alarm rate (P_f) is the probability of accepting H_1 given that H_o is true and the leakage rate (P_ℓ) is the probability of accepting H_o given that H_1 is true. The parameter d in the figure is signal-to-noise ratio related and defined as

$$d = \left[\sum_{\ell=1}^{k} a^2 s_o^2(t_\ell)\right]^{\frac{1}{2}}/\sigma. \qquad (21)$$

Here σ is set equal to 1 and a varies among .908, .454, .227 and .114 for the four curves shown. Each point on the performance curve corresponds to one value of the penalty factor η in the AIC defined by Eq. (5). The value of η is established by the actual operating point which is determined by the requirements for P_ℓ and P_f.

Now consider the case where there are two CSO's (n=2) separated by $\Delta\theta$ which is less than or equal to $2\lambda/d$ (one detector width). It is always assumed that the two targets are located at $\tau_1 = -\Delta\theta/2$ and $\tau_2 = \Delta\theta/2$, and σ is equal to 1. Fig. 5 shows the probabilities of identifying correctly, from a given observation, 2 targets, P(2), less than 2 targets, P(<2), and more than 2 targets, P(>2). The observation comes from two equally strong targets with signal-to-noise ratio (SNR*) of 10. The penalty factor, η is chosen as 3 here. The curves shown are drawn by connecting the

*The SNR of a target is defined as the intensity of the target at the center of its pulse shape divided by the RMS of the noise. The interference noise is not included.

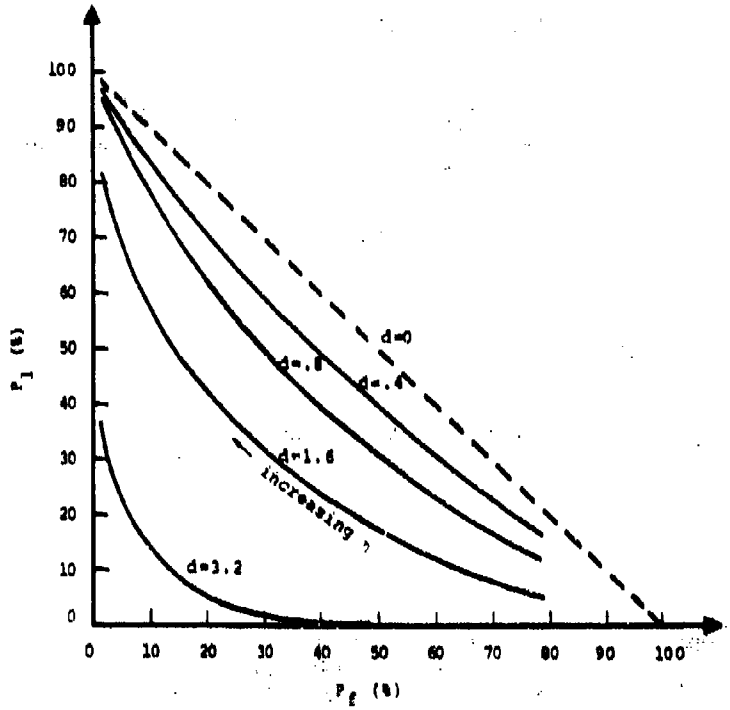

Fig. 4. Operation characteristic curve for the case where at most one target may exist.

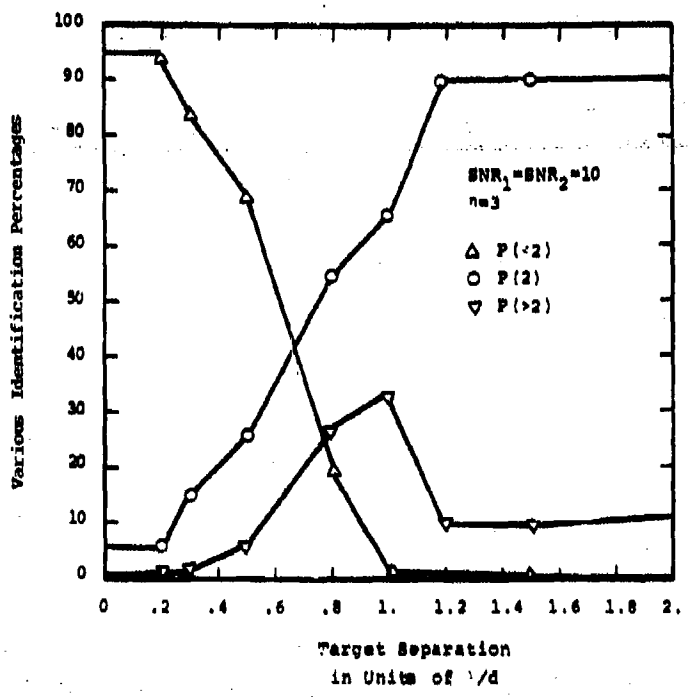

Fig. 5. Probabilities of identifying 2 targets P(2), less than 2 targets P(<2), and more than 2 targets P(>2), while the separation between the actual targets is varied.

finite simulation points. The probability of correctly identifying 2 targets is as high as 90% for separation, $\Delta\theta$, of $2\lambda/d$ (one detector width). However it is less than 25% for separations smaller than $.5\lambda/d$ (quarter of the detector width). The error is mainly because the 2 CSO's are identified as a single target. For separation, $\Delta\theta$, between $.5\lambda/d$ and λ/d, the correct detection rate is between 25% and 65%, and mis-detection is attributed to both under and over identifying the number of targets. The data at no separation ($\Delta\theta=0$) can be viewed from another angle. At $\Delta\theta=0$, the 2 CSO's are coincident and indistinguishable from a single target. Therefore, the data indicates that a single target with SNR=20 has 95% probability of being identified as a single target and 5% probability as 2 CSO's.

Fig. 6 illustrates the effect of choosing different values for the penalty factor η. It can be seen that using larger values of η can increase the detection rate for separation $\Delta\theta>\lambda/d$, but, at the expense of poorer performance for $\Delta\theta<\lambda/d$. There appears to be no obvious way to select η optimally. This does not contradict Akaike's theory because no proof for the optimality of using 2 for η, as proposed by Akaike, has been given. Although not shown in the figure, it is worthwile to point out that for $\eta=0$, P(2) is equal to 0% for any separation, $\Delta\theta$. In other words, the number of targets present is never correctly identified as 2 when the penalty term of the AIC statistics vanishes.

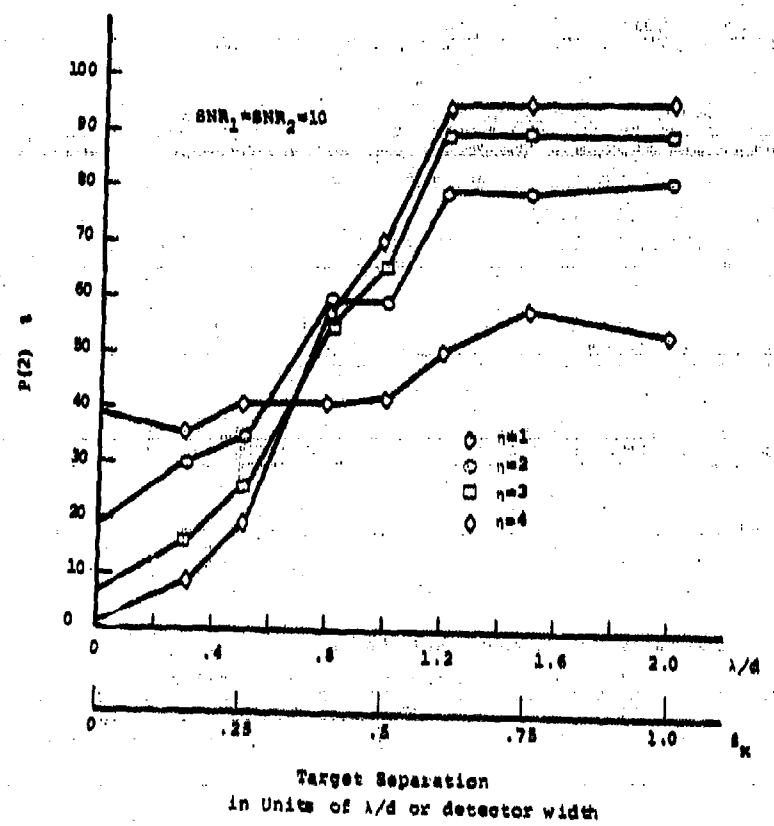

Fig. 6. Effect of choosing different values for the penalty factor in Eq. (11).

Fig. 7 shows P(2) as a function of $\Delta\theta$ for several different sets of target intensity. The variance of noise remains equal to 1. It is observed that the correct detection rate is generally higher for greater intensity except for the sudden drop of the top curve at $\Delta\theta=\lambda/d$. This drop in detection rate is due to the fact that in many of the 100 Monte Carlo runs for this case, the initial guess provided by the simulation algorithms causes the Quasi-Newton method to oscillate or to converge to a local maximum for the 2-target model but leads to a final estimation for the 3-target-model, which includes 2 targets close to the true ones and a third target of insignificant intensity. Note that an experimentor-supplied "good" initial guess for the 2-target model can bring up the detection rate at this point. As to why the algorithm fails at this particular point, no satisfactory explanation has been found.

In Fig. 5 the true model has 2-target with $a_1=a_2=9.08$ and $\tau_1=-\tau_2=-\Delta\theta/2$. Suppose the initial guess of the Quasi-Newton procedure is supplied by the experimentor instead of the algorithm itself and the experimentor intelligently selects $a_1^0=18.16, \tau_1^0=0$ for the initial guess of the 1-target model, $a_1{}^0=a_2{}^0=9.08$, $\tau_1{}^0=-\tau_2{}^0=-\Delta\theta/2$ for the 2-target model and $a_1{}^0=a_2{}^0=9.08$, $a_3{}^0=.1$, $\tau_1{}^0=-\tau_2{}^0=-\Delta\theta/2$, $\tau_3{}^0=0$ for the 3-target model. The resulting detection performance is shown in Fig. 8. A comparison of Figs. 5 and 8 shows that the "good" initial guess increases the correct

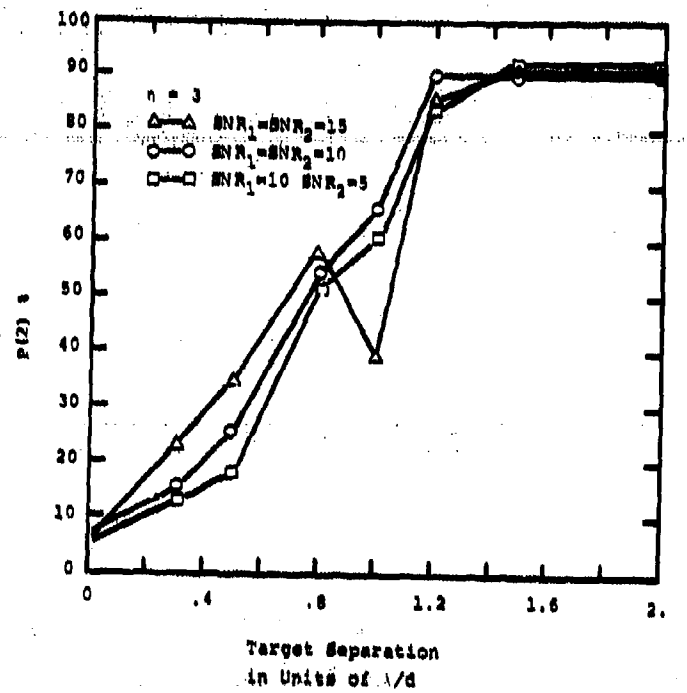

Fig. 7. Correct detection rate as function of target separation for several different sets of target intensities.

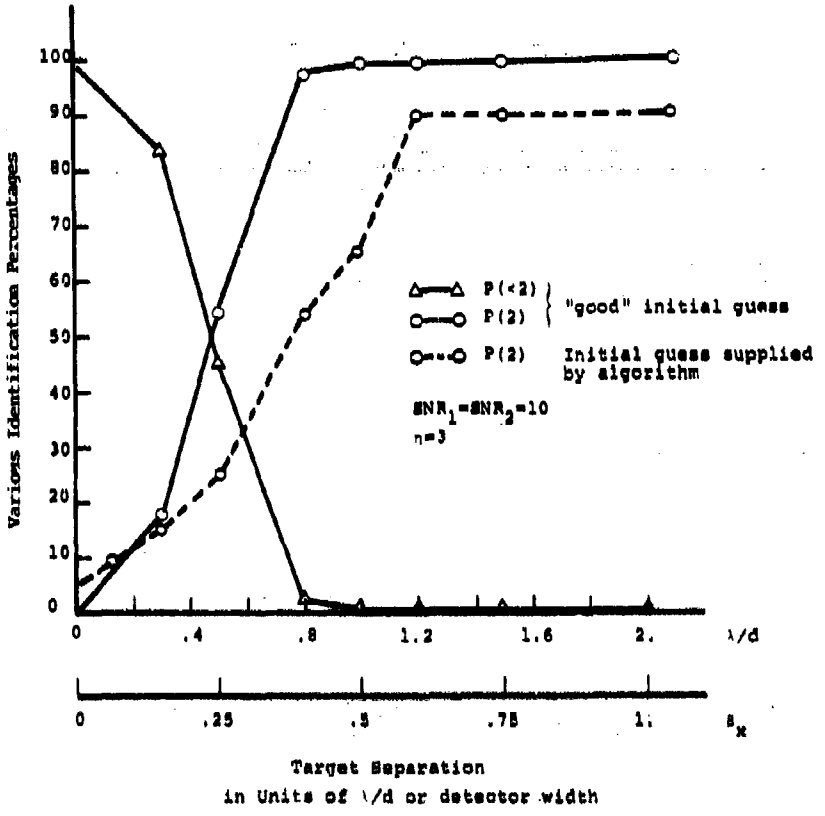

Fig. 8. Comparison of detection performance between using a "good" initial guess and using the initial guess provided by the simulation algorithm.

detection rate significantly. For separations as small as .8λ/d (two fifths of the detector width) the detection performance is almost perfect. The incorrect detection for even smaller separations is because only one target is recognized. The chance of identifying more than 2 targets is almost nil in the entire range of separations considered.

4.2 Estimation Performance

The performance of an estimator is usually evaluated in terms of estimation bias and variance. From the N simulation runs, the variance of an estimate is computed as

$$\sigma^2_{x_i} = \frac{1}{N} \sum_{j=1}^{N} (x_i^{(j)} - \bar{x}_i)^2 \qquad (22)$$

where $x_i^{(j)}$ is the estimate of the parameter x_i in the j^{th} run and

$$\bar{x}_i = \frac{1}{N} \sum_{j=1}^{N} x_i^{(j)} \qquad (23)$$

is the mean of the estimate. The bias of the estimate is then given by

$$b_{x_i} = \bar{x}_i - x_i \ . \qquad (24)$$

This sample variance can be compared with the Cramer-Rao

bound (CRB) which is a lower bound on the variance (or covariance matrix) of an unbiased estimator. In the case of a single target in additive white gaussian noise, the CRB for the estimation of parameter vector $\underline{x}$ can be obtained by

$$\sigma(x_i) = (F)^{-1}_{ii} \tag{25}$$

$$F_{ij} = \frac{1}{\sigma^2}\sum_{\ell=1}^{k}\frac{\partial s_d(t_\ell)}{\partial x_i}\,\frac{\partial s_d(t_\ell)}{\partial x_j} \tag{26}$$

where F is the Fisher information matrix, σ^2 the variance of the noise and $s_d(t)$ the desired signal. A set of discrete observations is assumed. This bound is usually tight when the signal-to-noise ratio is high.

Figs. 9 (a) and (b) compare the square roots of the $\sigma(x_i)$ and $\sigma^2_{x_i}$ for the intensity and postion respectively, in the case of two targets with SNR's both equal to 10. The angular separation between the two targets is the control variable. The simulation is only run at certain values of target separation. For the data shown in these figures the detection procedure is omitted by assuming that the number of targets present is known exactly in advance. That is to say a 2-target model is always assumed. The initial guess for this model is provided in two different ways for comparison. The first uses the procedure described in section 3.2 and the second relies on an "intelligent"

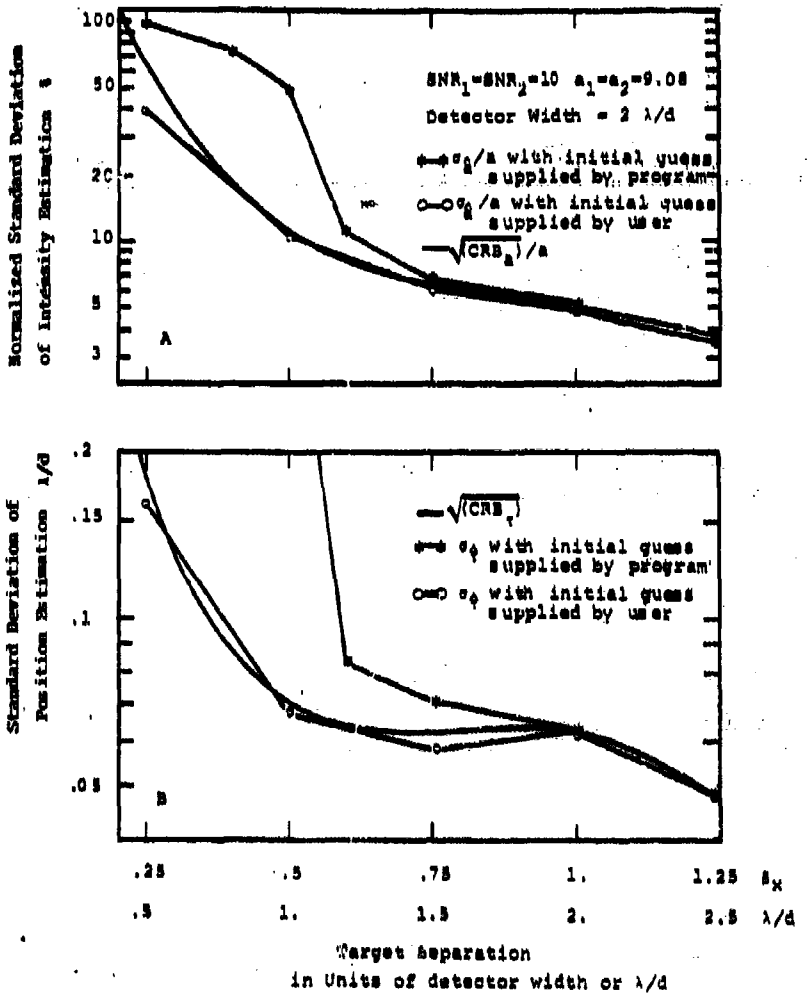

Fig. 9(a-b). Estimation performance and comparison; (a) intensity estimation, (b) position estimation; one example.

experimentor who selects the initial value of the parameter in the neighborhood of the true one.* Note that since $a_1=a_2$ and $|\tau_1|=|\tau_2|$, the concerned statistics for the first target should be very close to those for the second target and so no distinction between them is made in this figure.

From Fig. 9, it can be seen that when the initial guess is provided by the algorithm automatically, the estimate variance agrees with the CRB very well at target separations of $1.5\lambda/d$, $2\lambda/d$ and $2.5\lambda/d$. Recall that the observed signal exhibits two peaks for separation of $2.5\lambda/d$ as shown in Fig. 3(a). The sample variance is significantly larger than the CRB for separations less than $1.2\lambda/d$. When the "good" initial guesses are employed, the estimation variance becomes quite close to the CRB except at the point where separation, $\Delta\theta=.5\lambda/d$. This once again demonstrates the importance of the initial guess in an iterative optimization algorithm.

Figs. 10(a) and (b) show the same types of comparison as that of Figs. 9(a) and (b) for two targets with SNR's both equal to 15. Similar behaviors are observed. It should be pointed out the $\sqrt{C(\hat{a})}/a$ and $\sqrt{C(\hat{\tau})}$ of this example are smaller than those of the former example by a factor of 1.5, which is exactly equal to the ratio of the two corresponding SNR's.

*In the first case, the estimation procedure starts with the one-target model and ends with the two-target model. In the second case, it is only applied to the two-target model.

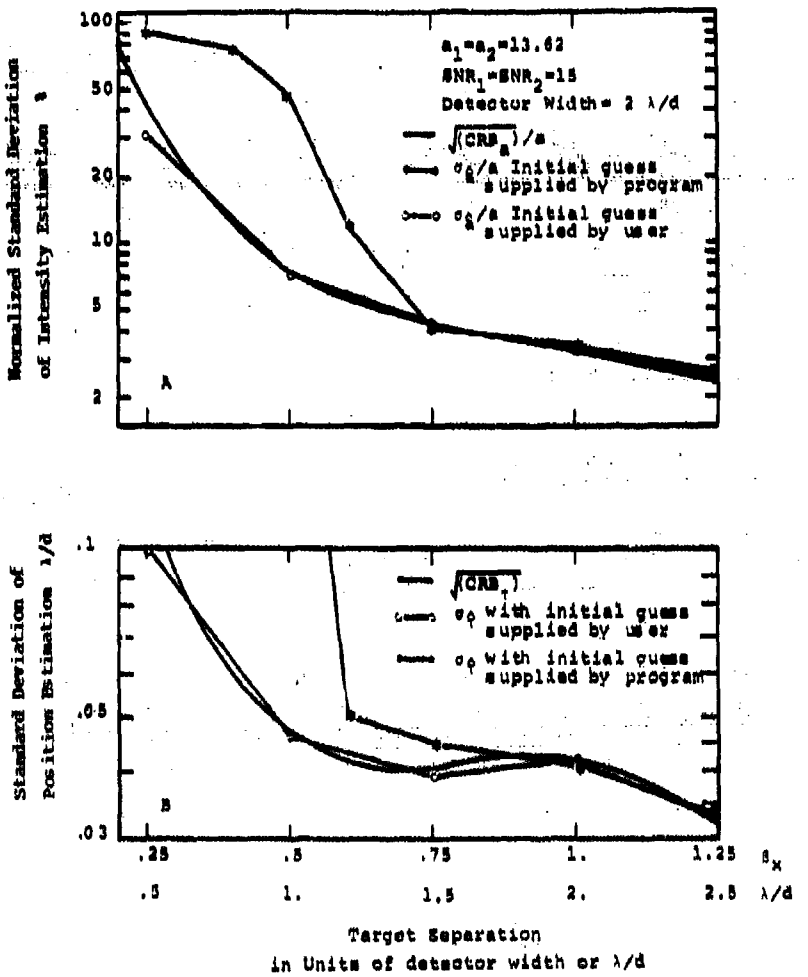

Fig. 10(a-b). Estimation performance and comparison, example.

Based on the same simulation as used in Fig. 9, the biases and the RMS errors* of the intensity and position estimations are shown in Fig. 11(a) and (b). Here the initial guess is generated by the estimator itself. It can be seen that the estimator is actually biased in the region where the sample variance deviates significantly from the Cramer-Rao bound. Meanwhile, the intensity bias, b_a, is relatively small compared to the corresponding sample standard deviation (roughly by an order) over the entire CSO region. However, at very small separation ($\leq 1\lambda/d$), the position bias is significant and contributive to total RMS error. If only those runs in which the number of targets is identified as 2 are used in computing the statistics, the bias, sample variance and RMS error can be recued slightly.

*The mean-square error e^2 is the sum of the variance and the squared bias $e^2=\sigma^2+b^2$.

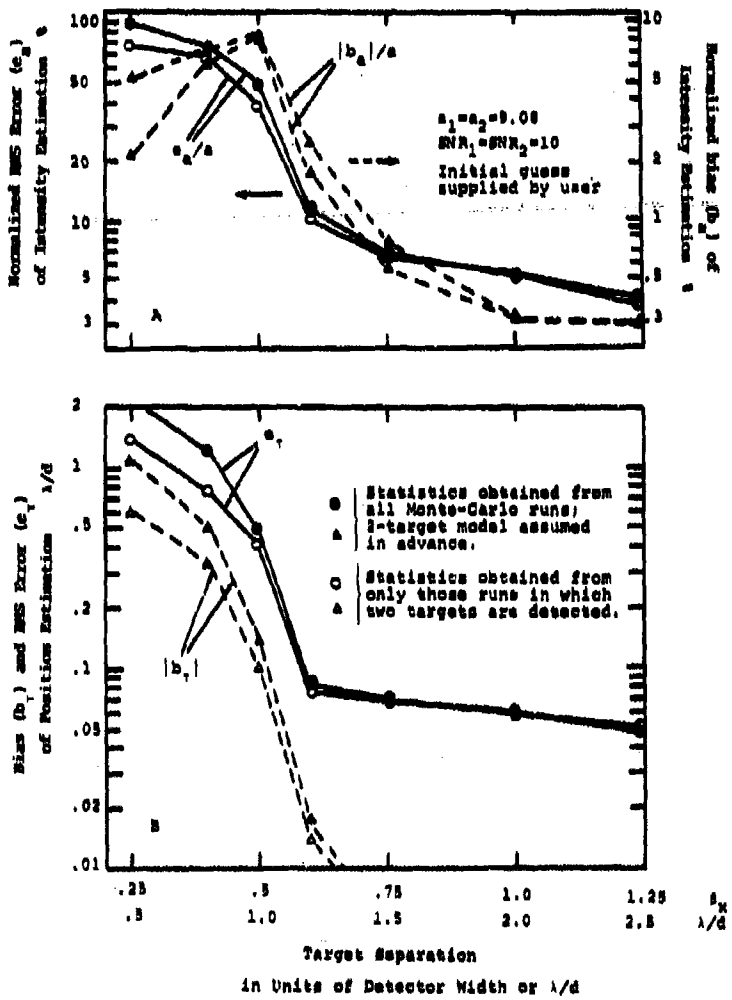

Fig. 11(a-b). Estimation bias and RMS error; (a) intensity estimation, (b) position estimation.

4.3 Discussion

In this simulation study, the pulse shape of the response of the photo-detector to a unit-intensity point target is assumed known exactly in advance. What the detection/estimation processor does is to adjust the intensities and positions of a certain number of ideal pulse shapes to best match this "synthesized" signal with the given observation. If the pulse shape is different from the one assumed in this report due to differences in aperture shapes, detector responses, detector configurations etc., the simulation program is still applicable as long as the pulse shape and its derivative can be made available. However, the performance of the detection and estimation process may vary significantly with different pulse shapes.

The algorithm described in this report is designed to process the CSO segments rather than the entire observation. It seems feasible to use this algorithm as the second stage of a two-stage signal processor which first process the original signal to identify the isolated "resolved" targets and to separate them from the potential CSO's. This approach may be quite efficient computationally if the probability of occurrence for CSO's is much lower than that of isolated targets.

One version of the Quasi-Newton method is implemented here for the optimization of the likelihood function. There exist some

other methods for this purpose, which can be divided into two general categories; the random method and the gradient method. Usually, no single method is best for all types of nonlinear optimization problems. No evaluation of different methods on the present CSO problem is undertaken in this report. However it is the author's feeling that selecting a particular optimization method may not be as important as devising an efficient and promising way to provide the initial guess.

A single scanning detector is assumed in this report. Since this detector can not resolve the cross-scan component of a target's position, the targets are assumed to lie along the in-scan direction. To determine the in-scan and cross-scan positions of a target, other detector configurations such as the chevron (a pair of detectors oriented in different directions) should be used.

In this simulation study, an additive white guassian noise is assumed. This assumption is valid when the thermal noise is the dominant noise source in the optical sensor system. However this noise model becomes inaccurate in the so-called shot-noise limited case where the noise level is dependent on the signal [3]. Even for this case, the detection/estimation scheme presented in this report can apply except that the likelihood function and its gradient should be reformulated. The mathematics involved is, of course, more complicated but still tractable.

V. CONCLUSION

In this report the detection and estimation problems of closely spaced optical point targets are studied using simulation. An annular aperture of 50% obscuration and a scanning photo-detector with in-scan and cross-scan dimensions equal to $2\lambda/d$ and $6\lambda/d$, respectively, are employed. The observed signal which originates from two point targets exhibits a single apparent peak when they are separated by less than one detector width. To detect and estimate such "unresolved" targets, the Akaike information criterion and a particular maximum likelihood estimator are utilized. The estimator is in fact a nonlinear estimation algorithm.

Several examples have been examined. It is found that for target separation between 3/4 and 1 detector width, the correct detection rate is fairly high, the estimator unbiased and the sampled variance close to the Cramer-Rao bound. However, the detection and estimation performances degrade significantly for smaller separations. This is unavoidable because when the two targets get closer they become more indistinguishable from a single target, particularly in the presence of noise. More importantly, the difficulty in providing algorithmically a "good" initial guess for the estimator contributes to the poor performance. Undoubtedly, the performance of the algorithm can be improved if a more intelligent way of choosing the initial guess can be devised.

APPENDIX A: COMPUTATIONAL ASPECTS

Programs have been written in accordance with the principles described in section 3 in order to simulate the detection/estimation processor. The performance of the processor is closely related to the particular implementations adopted. Therefore, before presenting the simulation results, the program actually used has to be specified more carefully. The top-level flow charts and details of some subroutines are given in this the following appendices.

A.1 Top-level Flow Charts

For practical reasons, the simulation is done in two steps by two different main programs. The first one (TABLE) is used to create the standard pulse shapes of $s_o(t)$ and $\dot{s}_o(t)$ in advance for use in the second one (CSOMCS) which is the program performing detection and estimation.

The top-level flow charts of these two programs are depicted in Figs. A1(a) and (b) respectively while their listings are given in the appendix. In these charts the functions of some blocks are implemented by subroutines. The names of these subroutines are put down beside the associated blocks. Some of them will be further explained in the following subsections. Note that the detection statistics are the output of the flow chart in Fig. A1.

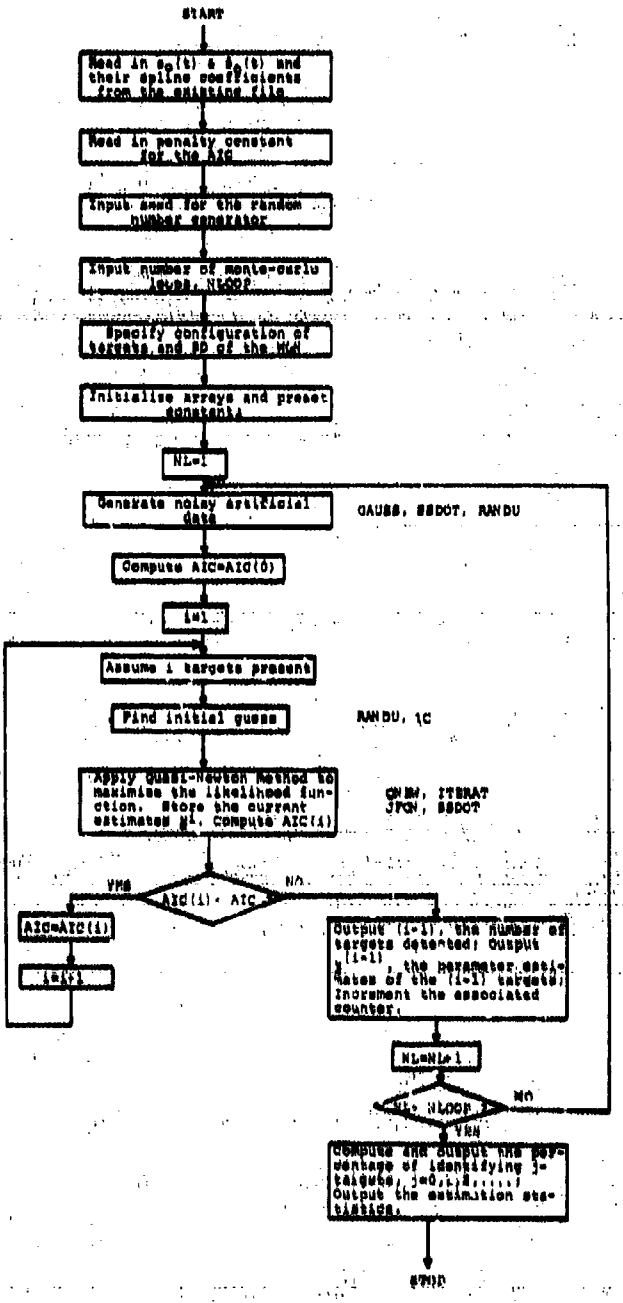

Fig. A1(a-b). Top-level flow charts of the simulation programs, CSOMCS (a) and TABLE (b).

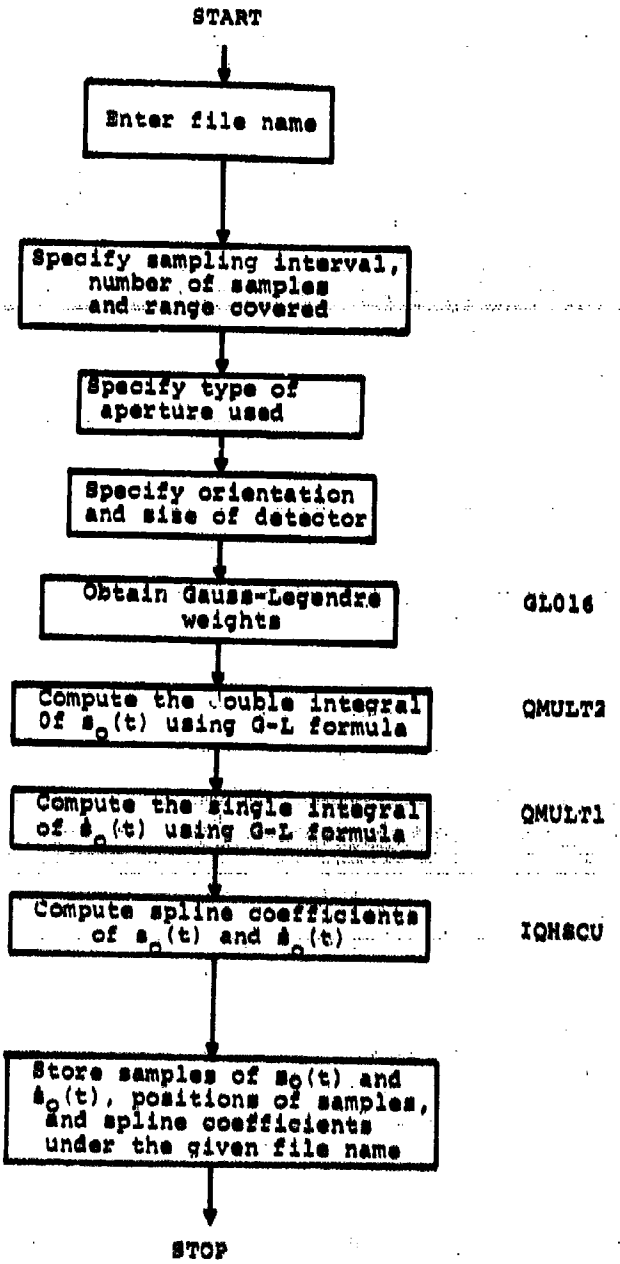

Fig. A1(a-b). Continued.

It can be modified easily to yield the estimation statistics.

A.2 Quasi-Newton Method

There are several versions of the so called Quasi-Newton method [8]. One particular version has been written by Dr. R. W. Miller in the Laboratory. This version is modified here to meet the requirements of the present simulation study. The procedures are as follows:

Step 1: Set k=0; read in the initial parameter values, $\underline{x}^0$, and the number of targets, n.

Step 2: Compute $J(\underline{x}^0)$ and $\nabla J(\underline{x}^0)$ according to Eqs. (12), (15) and (18). Find H^0 by inverting the matrix

$$G^0(i,j) = \frac{1}{d}\left[\frac{\partial J}{\partial x_j}(x_1^0,\ldots,x_i^0+d,\ x_{i+1}^0,\ldots,x_{2n}^0) - \frac{\partial J}{\partial x_j}(\underline{x}^0)\right] \quad i,j=1,2,\ldots,2n$$

where d is a fixed perturbation. If G^0 is uninvertable, H^0 is chosen as a diagonal matrix with

$$H^0(i,i) = d/||\nabla J(\underline{x}^0)||$$

where $||\cdot||$ is the Euclidean norm.

Step 3: Compute the increment of $\underline{x}^k$.

$$\Delta\underline{x}^k = H^k\, J(\underline{x}^k)$$

and its size,

$$c = ||\Delta\underline{x}^k||.$$

If c is less than a preset step size α, go to step 4. Otherwise, multiply $\Delta\underline{x}^k$ with α/c and set $c = \alpha$.

Step 4: Compute the increment of $J(\underline{x}^k)$,

$$\Delta J(\underline{x}^k) = \Delta\underline{x}^k \nabla J(\underline{x}^k).$$

If $\Delta J(\underline{x}^k)$ is positive, go to step 5. Otherwise, replace $\Delta\underline{x}^k$ with

$$\Delta\underline{x}^k = \beta \frac{\nabla J(\underline{x}^k)}{||\nabla J(\underline{x}^k)||}$$

where β is a preset number.

Step 5: Update $\underline{x}$,

$$\underline{x}^{k+1} = \underline{x}^k + \Delta\underline{x}^k$$

Step 6: Apply the range constraints, $-\frac{r}{2} \leq x_{n+j} \leq \frac{r}{2}$,

$j=1,\ldots,n$. For any j, if $|x_{n+j}^{k+1}| \leq \frac{r}{2}$ go to step 7. Otherwise, set

$$x_{n+j}^{k+1} = \begin{cases} -\frac{r}{2} & x_{n+j}^{k+1} < -\frac{r}{2} \\ \frac{r}{2} & x_{n+j}^{k+1} > \frac{r}{2} \end{cases}$$

and

$$\Delta x_{n+j}^k = x_{n+j}^{k+1} - x_{n+j}^k.$$

Recompute the magnitude of the increment,

$$c = ||\Delta \underline{x}^k||$$

Step 7: Compute $J(\underline{x}^{k+1})$, $\nabla J(\underline{x}^{k+1})$ and

$$H^{k+1} = H^k - \frac{(\Delta \underline{x}^k + H^k \underline{y}^k)(\Delta \underline{x}^k)^T H_k}{(\Delta \underline{x}^k)^T H_k \underline{y}_k}$$

provided the denominator is not equal to zero. Here,

$$\underline{y}^k = \nabla J(\underline{x}^{k+1}) - \nabla J(\underline{x}^k).$$

Step 8: If $c \leq c_o$, the iteration converges and $\underline{x}^k$ is the desired estimate. Stop. Otherwise proceed. Note that c_o is the threshold value of the stop criterion.

Step 9: If $k < k_o$, set $k = k+1$ and go to step 3. Otherwise, proceed to the following step. Here, k_o is a preset value for the maximum number of iterations.

Step 10: Among k_o iterations find the one which has the greatest value of $J(\underline{x}^k)$. Take the estimate of this iteration as the final estimate. Then stop.

The above procedures are implemented in subroutines QNEW and ITERAT. The necessary constants are preset for the simulation as $d = .005$, $\alpha = .5$, $\beta = .15$, $c_o = 10^{-5}$, and $k_o = 50$.

A.3 Computations of $s_o(t)$ and $\dot{s}_o(t)$

The Quasi-Newton procedure requires, at each iteration, the computations of $J(\underline{x})$ and $\nabla J(\underline{x})$ which, in turn, requires those of $s_o(t_\ell-\tau_i)$ and $\dot{s}_o(t_\ell-\tau_i)$ for $\ell=1,2,\ldots,k$ and $i=1,2,\ldots,n$. It is very time-consuming to directly carry out, for every iteration, the associated single and double integrals. Although the computation time can be reduced significantly by using the high-speed convolution method, it is still quite noticeable. An alternative approach is to compute in advance samples of $s_o(t)$ and $\dot{s}_o(t)$ as well as their spline coefficients, and store them in files. At the beginning of the simulation, those data are first retrieved and later on, whenever needed, $s_o(t_\ell-\tau_i)$ and $\dot{s}_o(t_\ell-\tau_i)$ can be computed by simple interpolations which take almost no time. If the number of stored samples is large enough, the interpolation would provide sufficient accuracy.

Since $s(t)$ and $\dot{s}_o(t)$ would be only computed once and off-line the computer time required is not critical. They are computed by directly carrying out the double and single intergrals of Eqs. (3) and (17) using the Gaussian-Legendre quadrature formula [10, 11]. This formula gives for the single integral,

$$I = \int_a^b f(u)du \qquad (A.1)$$

the following approximation

$$I = \frac{b-a}{2} \sum_{i=1}^{n} \left\{ A_i^{(n)} \cdot f\left(\frac{b-a}{2} x_i^{(n)} + \frac{b+a}{2} \right) \right\} \qquad (A.2)$$

where the weights $A_i^{(n)}$ and abscissas $x_i^{(n)}$ can be found from a standard mathematical table. The formula is exact whenever $f(u)$ is a polynomial of degree $\leq 2n-1$. The double integral of the form

$$I = \int_a^b \int_{\phi(v)}^{\psi(u)} f(u,v)\, du dv \qquad (A.3)$$

is approximated by

$$I = \frac{b-a}{2} \sum_{i=1}^{n} \left\{ A_i^{(n)} \cdot \frac{\psi(c_i)-\phi(c_i)}{2} \cdot \sum_{j=1}^{m} \left[A_j^{(m)} f\left(\frac{\psi(c_i)-\phi(c_i)}{2} x_j^{(m)} + \frac{\psi(c_i)+\phi(c_i)}{2}, c_i \right) \right] \right\} \qquad (A.4)$$

with

$$c_i = \frac{b-a}{2} x_i^{(n)} + \frac{b+a}{2} .$$

Here, both n and m are chosen equal to 16 for the current application, which is shown experimentally to be sufficient. Two subroutines QMULT2 and QMULT1 have been written for this purpose.

The spline coefficients used to interpolate the set of points from $s_o(t)$ (or $\dot{s}_o(t)$) are computed from the Quasi-Cubic Hermite splines [12]. The cubic spline representing the function between each pair of given points is determined by the coordinates and slopes at the two points. The slope at each point is determined

locally by the point in question and two points on its each side. The resulting curve passes through all the given points. The subroutine IQHSCU which is available in the IMSL package [13] is employed for this computation. The subroutine SSDOT called by the simulation main program performs the necessary interpolations to yield values of $s_d(t_\ell)$ (Eq. (2)) and $\partial s_d(t_\ell)/\partial x_i$ (Eq. (16)), for $\ell=1, 2,\ldots,k$ and $i=1, 2,\ldots,2n$ given any $\underline{a}$ and $\underline{\tau}$. Using the output of SSDOT the subroutine JFCN computes the desired $J(\underline{x})$ and $\nabla J(\underline{x})$.

A.4 Choice of Initial Guess

The subroutine IC is employed to provide the initial guess for the Quasi-Newton procedure. The associated principal logic has been described in subsection 3.2. In this subsection, the details of the program and the flow chart are given.

At the $(i+1)^{th}$ step of the AIC procedure, the initial guesses of the first i targets are set equal to the estimates from the i^{th} step and the initial guess for the $(i+1)^{th}$ target is found through the pure random search. From Eq. (12), it is clear that maximizing $J(\underline{x})$ is equivalent to minimizing the following function

$$\Phi_1 = \sum_{\ell=1}^{k}\left[y(t_\ell) - \sum_{j=1}^{i+1} a_j s_o(t_\ell-\tau_j)\right]^2 \qquad (A.5)$$

over a_j and τ_j, $j=1,\ldots,i+1$.

Since a_j and τ_j, j=1,...,i, are already fixed, it also becomes equivalent to minimizing

$$\phi_2 = \sum_{\ell=1}^{k} \left[y_1(t_\ell) - a_{i+1} s_o(t_\ell - \tau_{i+1}) \right]^2 \qquad (A.6)$$

over a_{i+1} and τ_{i+1}, where

$$y_1(t_\ell) = y(t_\ell) - \sum_{j=1}^{i} a_j s_o(t_\ell - \tau_j) \qquad (A.7)$$

is the residue of y(t) after being fit by the fixed i targets. Further assume that (a_{i+1}, τ_{i+1}) lies on the curve imposed by

$$\frac{\partial \phi_2}{\partial a_{i+1}} = 0,$$

i.e.,*

$$a_{i+1} = \frac{\sum_{\ell=1}^{k} s_o(t_\ell - \tau_{i+1}) y_1(t_\ell)}{\sum_{\ell=1}^{k} s_o^2(t_\ell - \tau_{i+1})} \qquad (A.8)$$

This leaves τ_{i+1} the only parameter to be searched for the minimization of ϕ_2. The number of random trials in searching for τ_{i+1} is selected equal to 50 in the program. The flow chart is shown in Fig. A2.

*Eq. (A.8) is the same as Eq. (13) with n=1.

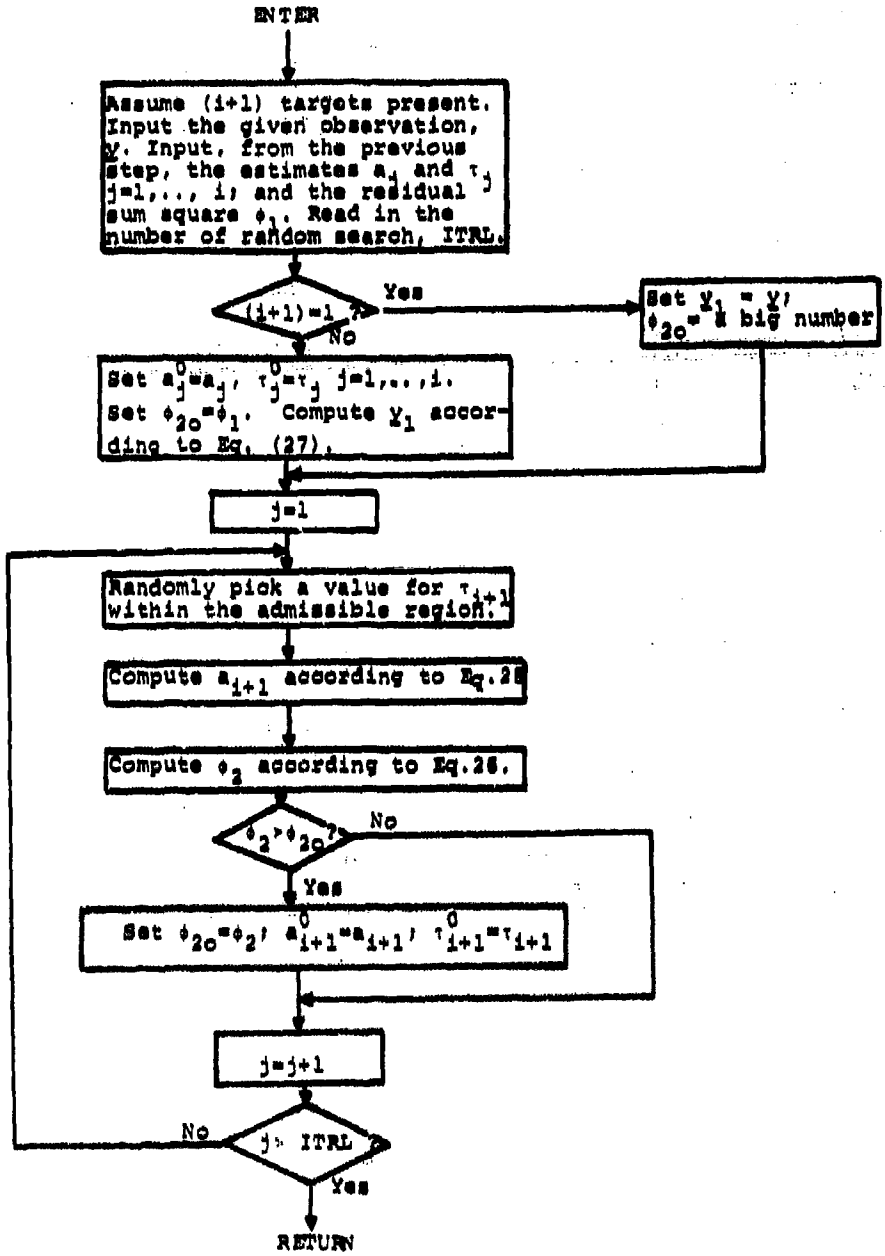

Fig. A2. Flow chart of the initial-guess generating subroutine.

APPENDIX B: PROGRAM LISTINGS

The whole simulation algorithm is composed of two main programs, TABLE and CSOMCS. The important input and output variables as well as the listings of these programs are given in this appendix. As for the detailed logic of the algorithm, readers should refer to the context of the report. The comments incorporated in the program will be also helpful in understanding the program.

Important Variables

TABLE:

IP = indicator of the type of aperture; 1 for square aperture and 2 for annular aperture

E = obscuration factor of the annular aperture; $0 \leq E < 1$

ANGLE = orientation of the detector, specified by the angle (degree) between the central line of the detector and the cross-scan direction; $0 \leq ANGLE \leq 90$.

NPOINT = number of points where values of $s_o(t)$ and $\dot{s}_o(t)$ are computed

TDELTA = interval between a pair of successive points in units of λ/d

TBEGIN = position of the first point, equal to (NPOINT-1) *TDELTA/2

ARG = array containing positions of the NPOINT points

VAL1 = array containing the corresponding NPOINT values of $s_o(t_i)$

VAL2 = array containing the NPOINT values of $\dot{s}_o(t_i)$

SPLIN1 = array of dimension NPOINTx3, containing the spline coefficients of $s_o(t_i)$

SPLIN2 = array of dimension NPOINTx3, containing the spline coefficients of $\dot{s}_o(t_i)$

FILEN = name of the file which keeps the necessary data (FILEN, TBEGIN, TDELTA, NPOINT, ARG, VAL1, VAL2, SPLIN1 and SPLIN2) for use in the simulation program CSOMCS

CSOMCS:

FILEN, TBEGIN, TDELTA, NPOINT, ARG, VAL1, VAL2, SPLIN1, SPLIN2 as defined above for the program TABLE.

The following parameters are specified in order to generate artificial noisy signal.

IX = seed of the random number generator

NLOOP = number of Monte Carlo simulation runs

NTO = number of targets present

NS = number of samples

DT = sampling interval

AMP = array containing intensities of the NTO targets

THETA = array containing positions of the NTO targets

STD = standard deviation of the WGN

BT = position of the first sample, equal to (NS-1)*DT/2

The following parameters are used in the detection/estimation procedure:

NT = number of targets assumed

N = total number of free parameters, equal to 2xNT

X = vector of length N. The intensity and position estimates of the i^{th} target are kept in x(i) and x(i+NT).

NM = preset upper bound of the number of assumed target

ETA = value of the AIC penalty constant

AIC = value of the Akaike information criterion

SSQ = value of $J(\underline{x})$ in Eq. (12)

SSQN = value of SSQ under the assumption that no target present

S = vector of length NS containing values of $s_{\underline{a}}(t)$ taken in the NS points

SDOT = vector of length NSxN containing partial derivatives of $s_d(t)$;

$\frac{\partial s_d(t_\ell)}{\partial a_1}, \ldots, \frac{\partial s_d(t_\ell)}{\partial a_{NT}}, \frac{\partial s_d(t_\ell)}{\partial \tau_1}, \ldots, \frac{\partial s_d(t_\ell)}{\partial \tau_{NT}}$ are

stored sequentially in the locations beginning at SDOT((ℓ-1)*N+1)

XBAR = vector containing mean values of the estimates in all the models assumed

XVAR = vector containing variances of the estimates

ICOUNT = array whose i^{th} element containing the probability of identifying i targets

EPS = smallest increment used in convergence test (for QNEW subroutine)

LIMIT = allowed largest number of iterations (for QNEW subroutine)

ITRL = number of the random searches used in subroution IC for choosing the initial guess

Listings

```
C
C*                MAIN TABLE
C
C --- DESCRIPTION:
C     THIS PROGRAM  COMPUTES AND STORES THE OPTICAL PULSE SHAPE AND
C      ITS FIRST DERIVATIVE W.R.T. ANGULAR POSITION FOR FUTURE USE.
C     THE SINGLE INTEGRAL OF EQ.(17) IS EVALUATED BY USING GAUSS-
C      LEGENDRE FORMULA. SUBROUTINE GL016 PROVIDES A TABLE OF THE 16-
C      POINT GAUSS-LEGENDRE FORMULA.
C     THE DOUBLE INTEGRAL OF EQ.(3) IS COMPUTED USING THE SAME METHOD.
C
      EXTERNAL FCN,FUP,FLO,FCT
      DOUBLE PRECISION DX(16),DA(16)
      DIMENSION X(16), A(16), FILEN(3)
      DIMENSION VAL1(1024),VAL2(1024),ARG(1024),SPLIN1(1024,3),SPLIN2(
     &1024,3)
      COMMON /PSF/ IP,E /DETOR/ CENTER,ANGLE,BETAX
      WRITE(6,10)
10    FORMAT(//10X,'*** TABLE ***'//)
      WRITE(6,20)
20    FORMAT(1X,'READ IN FILE NAME')
      READ(5,30) FILEN
30    FORMAT(3A4)
      WRITE(6,40) FILEN
40    FORMAT(1X,'FILE NAME=',3A4)
      TDELTA = .025
      NPOINT=1024
      RANGE = (NPOINT-1) * TDELTA
      TBEGIN = -RANGE /2.
      BETAX = 2.
      BETAY = 6.
      BETAYH = BETAY/2.
      BETAYL = -BETAYH
      WRITE(6,50)
50    FORMAT(1X,'READ IN IP: 1 FOR RECTANGULAR, 2 FOR ANNULAR ')
      READ(5,*) IP
      WRITE(6,60) IP
60    FORMAT (1X,'IP= ',I2)
      IF (IP .EQ. 1 ) GO TO 80
      WRITE(6,65)
65    FORMAT(1X,' READ IN  OBSCURATION FACTOR ')
      READ(5,*) E
      WRITE(6,70) E
70    FORMAT(1X,' E= ',F4.2)
80    WRITE(6,90)
90    FORMAT(1X,'READ IN DETECTOR ANGLE(DEGREE)')
      READ(5,*) ANGLE
      WRITE(6,100) ANGLE
100   FORMAT(1X,'ANGLE=',F6.2)
C
C OBTAIN THE GAUSS-LEGENDRE WEIGHTS
C
      CALL GL016(DX,DA,-1.D0, 1.D0 )
      DO 110 I=1,16
      X(I) = DX(I)
110   A(I) = DA(I)
      MM = 16
C
C COMPUTE THE PULSE SHAPE,VAL1 AND ITS DERIVATIVE VAL2
C
      DO 120 I=1,NPOINT
      CENTER = TBEGIN + TDELTA* (I-1)
```

```
      ARG(I) = CENTER
      VAL1(I) = QMULT2(FCN,BETAYL,BETAYH,FUP,FLO,X,A,MM)
      VAL2(I) = QMULT1(FCT,BETAYL,BETAYH,X,A,MM)
120   CONTINUE
C
C  COMPUTE THE SPLINE COEFFICIENT OF VAL1. SUB IQHSCU IS IN IMSL.
C
      CALL IQHSCU(ARG,VAL1,NPOINT,SPLIN1,NPOINT,IER)
C
C  COMPUTE THE SPLINE COEFFICIENT OF VAL2.
C
      CALL IQHSCU(ARG,VAL2,NPOINT,SPLIN2,NPOINT,IER)
C
C  WRITE OUT THE DATA
C
      WRITE(6,130) TBEGIN,TDELTA,NPOINT
130   FORMAT(/1X,2E14.7,I8/)
      DO 150 I=1,NPOINT
      WRITE(6,140) I,ARG(I),VAL1(I),VAL2(I),(SPLIN1(I,J),J=1,3),(SPLIN2(
     &I,J),J=1,3)
140   FORMAT(1X,I5,2X,9E12.5)
150   CONTINUE
C
C  STORE DATA UNDER THE GIVEN FILE NAME
C
      WRITE(8,160) FILEN,TBEGIN,TDELTA,NPOINT
      DO 170 I=1,NPOINT
      WRITE(8,180) ARG(I),VAL1(I),VAL2(I),(SPLIN1(I,J),J=1,3),
     1   (SPLIN2(I,J),J=1,3)
170   CONTINUE
160   FORMAT(3A4,2E14.7,I6)
180   FORMAT(9E14.7)
      STOP
      END



C*                FUNCTION QMULT2
C
C  COMPUTE THE DOUBLE INTEGRAL SS F(X,Y) DXDY, AA.LE.Y.LE.BB,
C  FL(Y).LE.X.LE.FU(Y)
C
      FUNCTION QMULT2(FCN,AA,BB,FU,FL,X,A,MM)
      DIMENSION X(1),A(1)
      H1 = (BB-AA)/2.
      G1 = (BB+AA)/2.
      Q1 = 0.
      DO 4 I=1,MM
      UI = H1*X(I) + G1
      AI = H1*A(I)
      D = FU(UI)
      C = FL(UI)
      H = (D-C)/2.
      G = (D+C)/2.
      Q = 0.
      DO 2 J=1,MM
      VJ = H*X(J) + G
2     Q = Q + A(J) * FCN(VJ,UI)
4     Q1 = Q1 + AI*H*Q
      QMULT2 = Q1
      RETURN
      END
```

```
C*                FUNCTION FCN
C
C  COMPUTE F(X,Y) WHICH IS USED IN QMULT2
C
      FUNCTION FCN(X,Y)
      DOUBLE PRECISION MMBSJ1,DR
      COMMON /PSF/ IP,E
      SCALE = 3.141593
      GO TO (10,20),IP
 10   IF (X .EQ. 0.) GO TO 32
      X1 = X * SCALE
      FX = (SIN(X1)/X1)**2
      GO TO 36
 32   FX=1.
 36   IF (Y .EQ. 0.) GO TO 42
      Y1 = Y* SCALE
      FY = (SIN(Y1)/Y1)**2
      GO TO 46
 42   FY =1.
 46   FCN = FX*FY
      RETURN
 20   R = SQRT(X**2 + Y**2 ) *SCALE
      IF (R .NE. 0.) GO TO 50
      FCN=1.
      RETURN
 50   DR=R
C
C  MMBSJ1 COMPUTES THE BESSEL FUNCTION OF FIRST KIND,EXISTING IN IMSL.
C
      BJ1=MMBSJ1(DR,IER1)
      IF(E.EQ.0.) GO TO 60
      DR=R*E
      BJ2=MMBSJ1(DR,IER2)
      GO TO 70
 60   IER2=0
      BJ2 = 0.
 70   IF (IER1 .NE. 0  .OR. IER2 .NE. 0) GO TO 80
      TEMP = 2./((1.-E**2)*R)
      FCN = ((BJ1 - E*BJ2) *TEMP)**2
      RETURN
 80   WRITE(6,90)
 90   FORMAT(//10X,' SUB MMBSJ1 ERROR ')
      CALL EXIT
      END


C*                FUNCTION FUP
C
C  THE UPPER BOUND USED IN QMULT2
C
      FUNCTION FUP(Y)
      COMMON /DETOR/ CENTER,ANGLE,BETAX
      FUP = CENTER + BETAX/2.
      IF(ANGLE.EQ.0.) GO TO 10
      FUP=FUP+Y*TAN(ANGLE*.01745329)
10    RETURN
      END
```

```
C*                FUNCTION FLO
C
C  THE LOWER BOUND USED IN QMULT2
C
      FUNCTION FLO(Y)
      COMMON /DETOR/ CENTER,ANGLE,BETAX
      FLO = CENTER - BETAX/2.
      IF(ANGLE.EQ.0.) GO TO 20
      FLO=FLO+Y*TAN(ANGLE*.01745329)
20    RETURN
      END


C*                FUNCTION QMULT1
C
C  COMPUTE THE SINGLE INTEGRAL S F(Y) DY
C
      FUNCTION QMULT1(FCT,AA,BB,X,A,MM)
      DIMENSION X(1),A(1)
      H1=(BB-AA)/2.
      G1=(BB+AA)/2.
      Q1=0.
      DO 4 I=1,MM
      UI=H1*X(I)+G1
      AI=H1*A(I)
4     Q1=Q1+AI*FCT(UI)
      QMULT1=Q1
      RETURN
      END


C*                FUNCTION FCT
C
C  COMPUTE F(Y) WHICH IS REQUIRED BY QMULT1
C
      FUNCTION FCT(Y)
      COMMON /DETOR/ CENTER,ANGLE,BETAX
      X=CENTER
      IF(ANGLE.EQ.0.) GO TO 30
      X = X + Y*TAN(ANGLE * .01745329)
30    X1 = X + BETAX/2.
      X2 = X - BETAX/2.
      FCT = FCN(X1,Y) - FCN(X2,Y)
      RETURN
      END


C*           SUBROUTINE GL016
C
C  PREPARE COEFFICIENTS OF THE 16-POINT GAUSS-LEGENDRE FORMULA
C
      SUBROUTINE GL016(X,A,C,D)
      DOUBLE PRECISION C,D,X(1),A(1),XX(8),AA(8)
      DATA XX/
     & .98940093499164993259615417340D0 ,
     & .94457502307323257607798841550D0 ,
     & .86563120238783174388046789770D0 ,
     & .75540440835500303389510119480D0 ,
     & .61787624440264374844667176400D0 ,
     & .45801677765722738634241944290D0 ,
     & .28160355077925891323046050140D0 ,
     & .95012509837637440185319335420-1 /
```

```
      DATA AA/
     & .27152459411754094851780572450-1,
     & .62253523938647892864384369900-1,
     & .95158511682492784809925107600-1,
     & .12462897125553387205247628210 ,
     & .14959598881657673208150173050 ,
     & .16915651939500253818931207900 ,
     & .18260341504492358886676366790 ,
     & .18945061045506849628539672320  /
      DMC = .5D0* (D-C)
      DPC = .5D0*(D+C)
      DO 2 I=1,8
      NI = 17-I
      X(I) = -DMC*XX(I) + DPC
      X(NI) = DMC*XX(I) + DPC
      A(I) = DMC*AA(I)
2     A(NI) = DMC*AA(I)
      RETURN
      END
```

```
C
C*                MAIN CSOMCS
C
C  ---  DESCRIPTION:
C     THIS PROGRAM IS A MONTE-CARLO SIMULATION OF THE INTENSITY AND ANGU
C  LAR LOCATION ESTIMATION OF CLOSELY SPACED OPTICAL TARGETS.
C     A SET OF ARTIFICIAL OBSERVATIONS ARE FIRST GENERATED FOR A GIVEN
C  CONFIGURATION (NO. OF TARGETS, INTENSITIES AND LOCATIONS).
C     USING THESE DATA AND ASSUMING NO. OF CSO'S,  A QAUSI-NEWTON ALGORI
C  THM IS EMPLOYED TO SEARCH FOR THE PARAMETER SET WHICH MAXIMUMS THE
C  LIKELIHOOD FUNCTION.
C     THE MEANS AND VARIANCES OF THE ESTIMATES ARE ALSO COMPUTED.
C     AKAIKE INFORMATION CRITERION IS COMPUTED FOR VARIOUS MODELS.
C
C
      INTEGER ICOUNT(5)
      REAL*4 AMP(4),THETA(4),X(8),S(64),SDOT(512)
      REAL*4 XBAR(20),XVAR(20),AML(100,5),DUM(8),TH(10),FILEN(3)
      COMMON  /DATA/Y(64),NS,STD /SAMPLE/BT,DT /WORK/SDOT
      COMMON /SPLINE/ TBEGIN,TDELTA,NPOINT,ARG(1024),VAL1(1024),VAL2(102
     1 4),SPLIN1(1024,3),SPLIN2(1024,3)
      WRITE(6,10)
      WRITE(6,20)
10    FORMAT(/5X,'*****     RESULTS FROM CSOMCS   *****')
20    FORMAT(10X,'CSO MONTE CARLO SIMULATION')
      WRITE(6,30)
30    FORMAT(14X,'WGN (STD UNKNOWN)')
C
C  READ IN STANDARD PULSE SHAPE FROM THE FILE WHICH HAS BEEN CREATED BY
C  PROGRAM TABLE.
C
      READ(8,50) FILEN,TBEGIN,TDELTA,NPOINT
      DO 40 I=1,NPOINT
      READ(8,60) ARG(I),VAL1(I),VAL2(I),(SPLIN1(I,J),J=1,3),
     1   (SPLIN2(I,J),J=1,3)
40    CONTINUE
50    FORMAT(3A4,2E14.7,I6)
60    FORMAT(9E14.7)
      WRITE(6,70) FILEN
70    FORMAT(/12X,'FILE NAME:',3A4/)
C     WRITE(6,*) TBEGIN,TDELTA,NPOINT
C     DO 12 I=1,NPOINT
C     WRITE(6,13) I,ARG(I),VAL1(I),VAL2(I),(SPLIN1(I,J),J=1,3),
C    &(SPLIN2(I,J),J=1,3)
C13   FORMAT(1X,I5,9E12.4)
C12   CONTINUE
      WRITE(6,80)
80    FORMAT(1X'ENTER THE PENALTY CONSTANT OF AIC')
      READ(5,*) ETA
      WRITE(6,90) ETA
90    FORMAT(2X,F5.2)
      WRITE(6,140)
140   FORMAT(' ENTER SEED FOR RANDOM NUMBER GENERATOR')
      READ(5,*) IX
      WRITE(6,150) IX
150   FORMAT(3X,I9)
      WRITE(6,160)
160   FORMAT(1X,'ENTER NO. OF MONTE-CARLO LOOPS')
      READ(5,*) NLOOP
      WRITE(6,170) NLOOP
170   FORMAT(3X,I4)
```

```
      WRITE(6,180)
180   FORMAT(' ENTER DATA TO GENERATE ARTIFICIAL SIGNAL:'/
     1   5X,'NT,NS,DELTA,AMP(NT),THETA(NT),STD')
      READ(5,*) NTO,NS,DT,(AMP(I),I=1,NTO),(THETA(I),I=1,NTO),STD
      WRITE(6,190) NTO,NS,DT,(AMP(I),I=1,NTO),(THETA(I),I=1,NTO),STD
190   FORMAT(1X,I3,I5,9F8.2)
      BT=-(NS-1)*DT/2.
      NM=NTO+1
      NM2=0
      DO 200 I=1,NM
200   NM2=NM2+I*2
      DO 210 I=1,NM2
      XBAR(I)=0.
210   XVAR(I)=0.
      NM1=NM+1
      DO 220 I=1,NM1
220   ICOUNT(I)=0
      EPS=1.E-5
      LIMIT=50
      ITRL=50
C
C  SIMULATE NOISELESS OBSERVATIONS
C
      CALL SSDOT(NTO,AMP,THETA,S,SDOT,NS,0)
      WRITE(6,230)
230   FORMAT(/' ESTIMATION STARTS: ')
      DO 400 NL=1,NLOOP
      WRITE(6,240) NL,IX
240   FORMAT(/1X,'NLOOP=',I4,5X,'IX=',I10)
C
C  SIMULATE ARTIFICIAL NOISY DATA
C
      DO 250 I=1,NS
      SMEAN = S(I)
      CALL GAUSS( IX,STD,SMEAN,Y(I))
250   CONTINUE
C
C   COMPUTE SSQ AND AIC FOR NT=0
C
      SSQN=0.
      DO 260 I=1,NS
260   SSQN=SSQN-Y(I)**2
C
C  VARIANCE OF THE NOISE IS UNKNOWN
C
      AIC=NS*ALOG(-SSQN/NS)
C
C  VARIANCE OF THE NOISE IS KNOWN
C     AIC=-SSQN/STD**2
C
      WRITE(6,270) SSQN,AIC
270   FORMAT(1X,'SSQN=',E15.6,5X,'AIC=',E15.6)
C
C   APPLY THE AIC PROCEDURE
C
      NT=1
280   N=NT*2
      WRITE(6,290) NT
290   FORMAT(I2,'-TARGET MODEL:')
      CALL IC(X,N,SSQ,IX,ITRL)
      WRITE(6,300) (  I),I=1,N)
300   FORMAT(1X,'IC: ,8E12.4)
```

```
C
C  USE B**2 FOR A SO THAT B IS NOT CONSTRAINED TO BE POSITIVE
C
      DO 310 I=1,NT
310   X(I)=SQRT(X(I))
      CALL QNEWT (X,N,SSQ,EPS,LIMIT,ITER,IER)
C
C  RESTORE A=B**2
C
      DO 320 I=1,NT
320   X(I)=X(I)**2
      CALL ORDER(X,N)
      WRITE(6,330) (X(I),I=1,N)
330   FORMAT(2X,'ESTIMATED PARAMETERS:',8E12.4)
C
C  VARIANCE IS UNKNOWN
C
      AICNT=NS*ALOG(-SSQ/NS) + ETA*(2*NT)
C
C  VARIANCE IS KNOWN
C     AICNT=-SSQ/STD**2 + ETA*(2*NT)
C
      WRITE(6,340) SSQ,AICNT,ITER
340   FORMAT(2X,'SSQ= ',E14.6,5X,'AIC=',E14.6,5X,'ITER.=',I4)
      IF(AICNT .GE. AIC) GOTO 360
      AIC=AICNT
      DO 350 I=1,N
350   DUM(I)=X(I)
      NT=NT+1
      IF (NT .GT. NM) GO TO 360
      GO TO 260
C
C  UPDATE THE COUNTER
C
360   ICOUNT(NT) = ICOUNT(NT) +1
      IF(NT .EQ. 1) GO TO 400
C
C  KEEP DATA FOR COMPUTING SAMPLE MEAN AND VARIANCE OF THE
C  ESTIMATED PARAMETERS
C
      K=0
      DO 370 I=2,NT
370   K=K+(I-2)*2
      N=(NT-1)*2
      DO 380 I=1,N
      XBAR(K+I)=XBAR(K+I)+DUM(I)
380   XVAR(K+I)=XVAR(K+I)+DUM(I)**2
400   CONTINUE
C
C  COMPUTE AND OUTPUT SIMULATION STATISTICS
C
      WRITE(6,410)
410   FORMAT(///1X'STATISTICS')
      NT=0
      WRITE(6,420)
420   FORMAT(2X,'0-TARGRT MODEL:')
      PCT=100.*ICOUNT(1)/FLOAT(NLOOP)
      WRITE(6,440) NT,PCT
      K=0
      DO 490 NT=1,NM
      N=NT*2
      WRITE(6,430) NT
430   FORMAT(/1X,I2,'-TARGET MODEL:')
```

```
      COUNT=FLOAT(ICOUNT(NT+1))
      PCT=COUNT/NLOOP*100.
      WRITE(6,440) NT,PCT
440   FORMAT(3X,'PROB(',I1,')=',F6.2,'%')
      IF(PCT.EQ.0.) GO TO 480
      DO 450 I=1,N
      I1=K+I
      XBAR(I1)=XBAR(I1)/COUNT
      XVAR(I1)=(XVAR(I1)-COUNT*XBAR(I1)**2)/COUNT
450   XVAR(I1)=SQRT(XVAR(I1))
      WRITE(6,460) (XBAR(K+I),I=1,N)
460   FORMAT(3X,'MEAN: ',8(1X,E12.4))
      WRITE(6,470) (XVAR(K+I),I=1,N)
470   FORMAT(3X,'STD: ',8(1X,E12.4))
480   K=K+N
490   CONTINUE
      CALL EXIT
      END


C*                SUBROUTINE QNEW
C
      SUBROUTINE QNEWT(X,N,XJ,EPS,LIMIT,ICONT,IER)
C
C  THIS SUBROUTINE IMPLEMENTS QUASI-NEWTON METHOD TO FIND A MAXIMUM OF
C  A FUNCTION.
C    X: INITIAL GUESS(INPUT); LOCATION OF MAXIMUM(OUTPUT)
C    N: DIMENSION OF X
C    XJ: VALUE OF MAXIMUM (OUTPUT)
C    EPS: SMALLEST INCREMENT USED IN CONVERGENCE TEST
C    LIMIT: MAXIMUM NUMBER OF ITERATIONS
C    ICONT: NUMBER OF ITERATIONS
C    IER: ERROR CODE
C  REQUIRES A SUBROUTINE JFCN(X,N,XJ,DJ) WHERE
C     X: ANY POINT IN THE PARAMETER SPACE
C     N: DIMENSION OF X AND DJ
C     XJ: VALUE OF THE FUNCTION AT X (OUTPUT)
C     DJ: GRADIENT EVALUATED AT X (OUTPUT)
C
      DIMENSION X(1),DJ(8),DJ1(8),X1(8)
      DIMENSION B(8,8),BI(8,8),FJ(51),FX(51,8)
      COMMON/MAIN1/NDIM/INOUT/KIN,KOUT
      COMMON/PARAM/S,DS,DSM,IOUT
C
C   MAX(N)=8, FJ(LIMIT+1), FX(LIMIT+1,N)
C  /MAIN1/ AND /INOUT/ ARE LINKED TO GMINV SUB.
C
      NDIM = 8
      KIN = 5
      KOUT = 6
C
C  FOLLOWING CONSTANTS ARE USED TO CONTROL NUMERICAL PROCEDURES OF QNEW
C    S: INITIALIZATION PERTURBATION
C    DS: INCREMENT USED WHEN NOT NEAR A MAXIMUM
C    DSM: LARGEST INCREMENT ALLOWED
C    IOUT=PRINTOUT CONTROL
C
      IOUT=1
      S=.005
      DS=.15
      DSM=.5
      IER = 0
```

```
      DO 10 I=1,N
10    FX(1,I)=X(I)
      CALL JFCN(X,N,XJ0,DJ)
      FJ(1)=XJ0
      IF(IOUT.GE.1) WRITE(6,20) XJ0
20    FORMAT(1X,'SSQ0=',E13.6)
C
C   INITIALIZE B
C
      DO 40 I=1,N
      DO 30 J=1,N
30    X1(J) = X(J)
      X1(I) = X(I) + S
      CALL JFCN(X1,N,XJ,DJ1)
      DO 40 J=1,N
40    BI(J,I) = (DJ1(J)-DJ(J))/S
      CALL GMINV(N,N,BI,B,MR,1)
      IF(MR.LT.N) GO TO 60
      DO 50 I=1,N
      DO 50 J=1,N
50    B(I,J) = -B(I,J)
      GO TO 100
C
C  ALTERNATE INITIALIZATION
C
60    DJM = 0.
      DO 70 I=1,N
70    DJM = DJM + DJ(I)**2
      DJM = S/SQRT(DJM)
      DO 90 I=1,N
      DO 80 J=1,N
80    B(I,J) = 0.
90    B(I,I) = DJM
C
C   ITERATE TO SOLUTION
C
100   DO 130 ICONT=1,LIMIT
      CALL ITERAT(X,B,DJ,XJ,DXN,N,IR)
      ICONT1=ICONT+1
      FJ(ICONT1)=XJ
      DO 110 I=1,N
110   FX(ICONT1,I)=X(I)
      IF(IOUT.GE.3) WRITE(6,120) ICOUNT,XJ,(X(I),I=1,N)
120   FORMAT(1X,I4,2E12.4,4E12.4/(29X,4E12.4))
      IF(IR.NE.0) GO TO 150
      IF(DXN.LT.EPS) GO TO 190
130   CONTINUE
      IF(IOUT.GE.1) WRITE(6,140) LIMIT
      IER = 2
140   FORMAT(2X,'NO CONVERGENCE IN',I4,' ITERATIONS')
      GO TO 160
150   IER=3
160   XJ=FJ(1)
      KMAX=1
      DO 170 I=2,ICONT1
      IF(FJ(I).LE.XJ) GO TO 170
      XJ=FJ(I)
      KMAX=I
170   CONTINUE
      DO 180 I=1,N
180   X(I)=FX(KMAX,I)
      RETURN
```

```
190   IF(XJ.GE.XJO) RETURN
      IER = 1
      IF(IOUT.GE.1) WRITE(6,200)
200   FORMAT(1X'NOT GLOBAL MAXIMUM')
      RETURN
      END


C*                SUBROUTINE ITERAT
C
C  CALLED BY QNEW
C
      SUBROUTINE ITERAT(X,B,F,XJ,DXN,N,IR)
      DIMENSION X(1),B(8,8),F(1),DF(8),DX(8),BF(8),DXB(8)
      COMMON/PARAM/S,DS,DSM,IOUT /SAMPLE/BT
      IR=0
      DXN = 0.
      DO 20 I=1,N
      DX(I) = 0.
      DO 10 J=1,N
10    DX(I) = DX(I) + B(I,J)*F(J)
20    DXN = DXN + DX(I)**2
      DXN = SQRT(DXN)
      IF(DXN.LE.DSM) GO TO 50
C
C INCREMENT TOO BIG
C
      DO 30 I=1,N
30    DX(I) = DX(I)*DSM/DXN
      DXN = DSM
      IF(IOUT.GE.3) WRITE(6,40)
40    FORMAT(' INCREMENT TOO BIG')
C
C CHECK FOR CORRECT MOTION
C
50    XDF = 0.
      DO 60 I=1,N
60    XDF = XDF + DX(I)*F(I)
      IF(XDF.GT.0.) GO TO 100
C
C MOTION IN WRONG DIRECTION;  CHANGE TO THE DIRECTION OF GRADIENT
C
      IF(IOUT.GE.3) WRITE(6,70)
70    FORMAT(' NEAR MINIMUM')
      FM = 0.
      DO 80 I=1,N
80    FM = FM + F(I)**2
      DXN = DS
      FM = DS/SQRT(FM)
      DO 90 I=1,N
90    DX(I) = FM*F(I)
100   DO 110 I=1,N
110   X(I) = X(I) + DX(I)
C
C  CONSTRAINT THE TARGET POSITIONS WITHIN THE RANGE (BT,-BT)
C
      NT1=N/2+1
      IFLAG=0
      DO 120 I=NT1,N
      ABSX=ABS(X(I))
```

```
      IF(ABSX.LE.-BT) GO TO 120
      IFLAG=1
      SIGNX=X(I)/ABSX
      TEMP=-SIGNX*BT
      DX(I)=DX(I)+TEMP-X(I)
      X(I)=TEMP
120   CONTINUE
      IF(IFLAG.EQ.0) GO TO 150
      DXN=0.
      DO 130 I=1,N
130   DXN=DXN+DX(I)**2
      IF(DXN.NE.0.) GO TO 140
      IR=1
      XJ=-1.E75
      RETURN
140   DXN=SQRT(DXN)
150   CALL JFCN(X,N,XJ,DF)
      DO 160 I=1,N
      DF(I) = DF(I) - F(I)
160   F(I) = DF(I) + F(I)
      DO 170 I=1,N
      BF(I) = 0.
      DXB(I) = 0.
      DO 170 J=1,N
      BF(I) = BF(I) + B(I,J)*DF(J)
170   DXB(I) = DXB(I) + DX(J)*B(J,I)
      A1 = 0.
      DO 180 I=1,N
180   A1 = A1 + DX(I)*BF(I)
      IF(A1.NE.0.) GO TO 190
      IR=2
      RETURN
190   A1 = 1./A1
      DO 200 I=1,N
      DO 200 J=1,N
200   B(I,J) = B(I,J) - A1*(BF(I)+DX(I))*DXB(J)
      IF(IOUT.GE.4) WRITE(6,210) ((B(J,I),I=1,N),J=1,N)
210   FORMAT(2E20.4)
      RETURN
      END



C*                SUBROUTINE GAUSS
C
C  GENERATE GAUSSIAN DISTRIBUTION RANDOM NOISE
C
      SUBROUTINE GAUSS(IX,S,AM,V)
      A=0.
      DO 10 I=1,12
      CALL RANDU(IX,IY,Y)
      IX=IY
10    A = A + Y
      V = (A-6.0) *S +AM
      RETURN
      END
```

```
C*                SUBROUTINE JFCN
C
C  COMPUTE  J(X) AND ITS GRADIENTS
C
C
      SUBROUTINE JFCN (X,N,SSQ,DJ)
      DIMENSION AMP(4),THETA(4),X(1),DJ(1),S(64),SDOT(512)
      COMMON  /DATA/ Y(64),NS,STD /WORK/SDOT,S
      NT=N/2
      DO 10 K=1,NT
      AMP(K)=X(K)**2
10    THETA(K)=X(K+NT)
      CALL SSDOT (NT,AMP,THETA,S,SDOT,NS,1)
      SSQ=0.
      DO 20 JL=1,NS
      BML = Y(JL) -S(JL)
      SSQ= SSQ-BML**2
20    CONTINUE
      DO 40 IR=1,N
      SUM=0.
      DO 30 JL=1,NS
      NN=N*(JL-1) + IR
      BML = Y(JL) -S(JL)
      SUM=SUM+SDOT(NN)*BML
30    CONTINUE
C
C  VARIANCE IS UNKNOWN
C
      DJ(IR)=-SUM/SSQ*NS
C
C  VARIANCE IS KNOWN
C
C     DJ(IR)=SUM/STD**2
40    CONTINUE
      RETURN
      END
```

```
C*                SUBROUTINE ORDER
C
C  ARRANGE THE ORDER OF THE TARGETS ACCORDING TO THEIR IN-SCAN POSITIONS
C
      SUBROUTINE ORDER(X,N)
      DIMENSION X(1)
      NT=N/2
      IF(NT.LE.1) RETURN
      I1=NT+1
      I2=N-1
      DO 20 I=I1,I2
      J1=I+1
      DO 10 J=J1,N
      IF(X(J).LE.X(I)) GO TO 10
      TEMP=X(I)
      X(I)=X(J)
      X(J)=TEMP
      TEMP=X(I-NT)
      X(I-NT)=X(J-NT)
      X(J-NT)=TEMP
10    CONTINUE
20    CONTINUE
      RETURN
      END
```

```
C*                SUBROUTINE IC
C
C  PROVIDE INITIAL GUESS FOR QNEW
C
      SUBROUTINE IC(X,N,SSQ,IX,ITRL)
      DIMENSION X(1),S(64),SDOT(512),Y1(64)
      COMMON /SAMPLE/BT /WORK/SDOT,S /DATA/Y(64),NS
      NT=N/2
      AL=BT
      AU=-BT
      IF(NT.NE.1) GO TO 20
      XJ0=1.E75
      DO 10 I=1,NS
10    Y1(I)=Y(I)
      GO TO 50
20    XJ0=-SSQ
      NT1=NT-1
      CALL SSDOT(NT1,X(1),X(NT),S,SDOT,NS,0)
      DO 30 I=1,NS
30    Y1(I)=Y(I)-S(I)
      DO 40 I=1,NT1
40    X(N-I)=X(N-I-1)
50    IFLAG=0
      DO 90 K=1,ITRL
      CALL RANDU(IX,IY,FY)
      IX=IY
      THETA=AL+(AU-AL)*FY
      CALL SSDOT(1,1.,THETA,S,SDOT,NS,0)
      SUM1=0.
      DO 60 I=1,NS
60    SUM1=SUM1+S(I)**2
      SUM2=0.
      DO 70 I=1,NS
70    SUM2=SUM2+S(I)*Y1(I)
      AMP=SUM2/SUM1
      IF(AMP.LT.1.E-6) AMP=1.E-6
      XJ=0.
      DO 80 I=1,NS
80    XJ=XJ+(Y1(I)-S(I)*AMP)**2
      IF(XJ.GE.XJ0) GO TO 90
      IFLAG=1
      X(NT)=AMP
      X(NT*2)=THETA
      XJ0=XJ
90    CONTINUE
      IF(IFLAG.EQ.1) GO TO 100
      X(NT)=1.E-6
      X(NT*2)=0.
100   RETURN
      END


C*          SUBROUTINE SSDOT
C
C  COMPUTE S(T) AND ITS DERIVATIVE AT NS INSTANTS
C
C
      SUBROUTINE SSDOT(NT,AMP,THETA,S,SDOT,NS,IFLAG)
      REAL*4 S(1),SDOT(1),AMP(1),THETA(1)
      COMMON /SAMPLE/BT,DT
      COMMON /SPLINE/ TBEGIN,TDELTA,NPOINT,ARG(1024),VAL1(1024),
     1   VAL2(1024),SPLIN1(1024,3),SPLIN2(1024,3)
```

```
C
C  IF IFLAG=0, SDOT IS NOT COMPUTED
C
      IF(NT.EQ.0) GO TO 20
      N = NT*2
      DO 10 I=1,NS
      S(I) =0.
      I1 = (I-1) * N
      TI=BT+(I-1)*DT
      DO 10 K=1,NT
      T =TI - THETA(K)
      KT = IFIX((T-TBEGIN)/TDELTA) + 1
      D = T-ARG(KT)
      S1 =((SPLIN1(KT,3) * D + SPLIN1(KT,2))
     1     *D + SPLIN1(KT,1)) * D + VAL1(KT)
      S(I) = S(I) + S1*AMP(K)
      IF(IFLAG .EQ. 0) GO TO 10
      K1=I1 + K
C
C  SDOT(K1) IS THE DERIVATIVE OF S W.R.T. B INSTEAD OF A. A=B**2
C
      SDOT(K1) = S1 * 2.*SQRT(AMP(K))
      K2 = K1+NT
      S2 = ((SPLIN2(KT,3)*D + SPLIN2(KT,2))
     1    *D + SPLIN2(KT,1)) *D+ VAL2(KT)
      SDOT(K2) =-AMP(K)*S2
10    CONTINUE
      RETURN
20    NM=NT*2*NS
      DO 30 I=1,NS
30    S(I)  =0.
      DO 40 I=1,NM
40    SDOT(I)= 0.
      RETURN
      END


C*                SUBROUTINE GMINV
C
C  MATRIX INVERSION ROUTINE
C
C
      SUBROUTINE GMINV(NR,NC,A,U,MR,MT)
C
C  MATRIX INVERSION ROUTINE
C         INPUT :
C         NR,NC =ROW AND COLUMN DIMEN. OF A
C         A     =MATRIX TO BE INVERTED
C         MT      = PRINT CONTROL VARIABLE
C         OUTPUT :
C         U = GENERALIZED INVERSE OF A
C         MR  = RANK OF U
C
      EXTERNAL DOT
      DIMENSION A(1),U(1),S(30)
      COMMON/MAIN1/NDIM
      COMMON/INOUT/KIN,KOUT
      NDIM1 = NDIM+1
      TOL = 1.E-14
      ADV = 1.E-24
      MR = NC
```

```
      NRM1 = NR-1
      TOL1 = 0.
      JJ = 1
      DO 10 J=1,NC
      S(J) = DOT(NR,A(JJ),A(JJ))
      IF (S(J) .GT. TOL1) TOL1=S(J)
10    JJ =JJ +NDIM
      TOL1 = ADV* TOL1
      ADV = TOL1
      JJ=1
      DO 100 J=1,NC
      FAC = S(J)
      JM1 =J-1
      JRM = JJ+NRM1
      JCM = JJ+JM1
      DO 20 I=JJ,JCM
20    U(I) = 0.
      U(JCM)=1.0
      IF( J .EQ. 1) GO TO 54
      KK=1
      DO 30 K=1,JM1
      IF (S(K) .EQ. 1.0) GO TO 30
      TEMP= -DOT(NR,A(JJ),A(KK))
      CALL VADD(K,TEMP,U(JJ),U(KK))
30    KK=KK+NDIM
      DO 50 L=1,2
      KK=1
      DO 50 K=1,JM1
      IF (S(K) .EQ. 0.) GO TO 50
      TEMP =-DOT(NR,A(JJ),A(KK))
      CALL VADD(NR,TEMP,A(JJ),A(KK))
      CALL VADD(K,TEMP,U(JJ),U(KK))
50    KK = KK+NDIM
      TOL1 =TOL *FAC+ADV
      FAC = DOT(NR,A(JJ),A(JJ))
54    IF (FAC .GT. TOL1) GOT O 70
      DO 55 I=JJ,JRM
55    A(I) =0.
      S(J) =0.
      KK = 1
      DO 65 K=1,JM1
      IF (S(K) .EQ. 0.) GO TO 65
      TEMP =-DOT(K,U(KK),U(JJ))
      CALL VADD (NR,TEMP,A(JJ),A(KK))
65    KK = KK+NDIM
      FAC =DOT(J,U(JJ),U(JJ))
      MR =MR-1
      GO TO 75
70    S(J) =1.0
      KK=1
      DO 72 K=1,JM1
      IF (S(K) .EQ. 1.) GO TO 72
      TEMP= -DOT(NR,A(JJ),A(KK))
      CALL VADD(K,TEMP,U(JJ),U(KK))
72    KK=KK+NDIM
75    FAC =1./SQRT(FAC)
      DO 80 I=JJ,JRM
80    A(I) = A(I) * FAC
      DO 85 I=JJ,JCM
85    U(I)=U(I)*FAC
100   JJ=JJ+NDIM
      IF (MR .EQ. NR .OR. MR.EQ.NC) GO TO 120
```

```
      IF (MT .NE. 0)WRITE(KOUT,110)NR,NC,MR
110   FORMAT(I3,1HX,I2,8H M: RANK,I2)
120   NEND =NC*NDIM
      JJ=1
      DO 135 J=1,NC
      DO 125 I=1,NR
      II=I-J
      S(I)=0.
      DO 125 KK=JJ,NEND,NDIM
125   S(I)=S(I)+A(II+KK)*U(KK)
      II=J
      DO 130 I=1,NR
      U(II)=S(I)
130   II=II+NDIM
135   JJ=JJ+NDIM1
      RETURN
      END

C
C
      SUBROUTINE VADD(N,C1,A,B)
C         INPUT :
C         N = ARRAY DIMENSION
C         C1 = SCALAR
C         A = NX1 CECTOR
C         B = NX1 VECTOR
C         OUTPUT :
C         A = NX1 VECTOR SUM
      DIMENSION A(1),B(1)
      DO 1 I=1,N
1     A(I) =A(I) +C1*B(I)
      RETURN
      END

      FUNCTION DOT(NR,A,B)
C         INPUT :
C         NR = ARRAY DIMENSION
C         A = NRX1 VECTOR
C         B = NR X! VECTOR
      DIMENSION A(1),B(1)
      DOT =0.
      DO 1 I=1,NR
1     DOT=DOT + A(I)*B(I)
      RETURN
      END
```

ACKNOWLEDGMENTS

The critical comments and careful reviews of Drs. J. A. Tabaczynski, S. D. Weiner and K. P. Dunn are gratefully acknowledged. The author also wish to thank F. Chen for her assistance in computer programming. In addition, the skillful typing of the manuscript by C. A. Lanza is appreciated.

REFERENCES

1. R. W. Miller, "Accuracy of Parameter Estimates for Unresolved Objects," Technical Note 1978-20, Lindoln Laboratory, M.I.T. (8 June 1978), DDC AD-B028168.

2. D. L. Fried, "Resolution, Signal-to-Noise Ratio and Measurements Precision," Optical Science Consultants, Report No. TR-034, (October 1971), also published in J. Opt. Soc. Am., 69, 339 (1979).

3. M-J. Tsai and K-P. Dunn, "Performance Limitation of Parameter Estimation of Closely Spaced Optical Targets Using Shot-Noise Detector Model," Technical Note 1979-35, Lincoln Laboratory M.I.T. (13 June 1979), DDC AD-A073462.

4. K-P. Dunn, "Accuracy of Parameter Estimates for Closely Spaced Optical Targets," Technical Note 1979-43, Lincoln Laboratory, M.I.T. (13 June 1979), DDC AD-A073093.

5. H. Akaike, "A New Look at the Statistical Model Identification," IEEE Trans. Automat. Contr. AC-19, 716 (1974).

6. A. Papoulis, System and Transformation with Application in Optics (McGraw-Hill, New York, 1968).

7. M. Kaveh, "A Modified Akaike Information Criterion," Proc. 1978 IEEE Conference on Decision and Control, 949, San Diego, CA. (January 1979).

8. J. E. Dennis, Jr. and J. J. More, "Quasi-Newton Methods, Motivation and Theory," SIAM Review 19, pp. 46-89 (1977).

9. S. H. Brooks, "A Discussion of Random Methods for Seeking Maxima," Operation Research 6, pp. 244-251 (April 1958).

10. V. I. Krylov, Approximate Calculation of Integrals (MacMillan, New York, 1962).

11. A. H. Stoud, Approximate Calculation of Multiple Integrals (Prentice-Hall, Englewood Cliffs, NJ, 1971).

12. H. Akima, "A New Method of Interpolation and Smooth Curve Fitting Based on Local Procedure," JACM 17, pp. 589-602, (1970).

13. IMSL Computer Subroutine Libraries in Mathematics and Statistics, Sixth edition, (Internation Mathematical & Statistical Libraries, Inc. Houston, Texas, 1977).

UNCLASSIFIED

SECURITY CLASSIFICATION OF THIS PAGE (When Data Entered)

14 TN 1980-19

19

REPORT DOCUMENTATION PAGE

READ INSTRUCTIONS BEFORE COMPLETING FORM

1. REPORT NUMBER: ESD-TR-80-23 (18)	2. GOVT ACCESSION NO.: AD-A088098
3. RECIPIENT'S CATALOG NUMBER	
4. TITLE (and Subtitle): Simulation Study on Detection and Estimation of Closely Spaced Optical Targets (6)	5. TYPE OF REPORT & PERIOD COVERED: Technical Note (9)
6. PERFORMING ORG. REPORT NUMBER: Technical Note 1980-19	
7. AUTHOR(s): Ming-Jer Tsai (10)	8. CONTRACT OR GRANT NUMBER(s): F19628-80-C-0002 (15)
9. PERFORMING ORGANIZATION NAME AND ADDRESS: Lincoln Laboratory, M.I.T. P.O. Box 73 Lexington, MA 02173	10. PROGRAM ELEMENT, PROJECT, TASK AREA & WORK UNIT NUMBERS: Program Element Nos. 63304A and 63308A
11. CONTROLLING OFFICE NAME AND ADDRESS: Ballistic Missile Defense Program Office Department of the Army 5001 Eisenhower Avenue Alexandria, VA 22333 (11)	12. REPORT DATE: 18 March 1980 (12) 79
	13. NUMBER OF PAGES: 80
14. MONITORING AGENCY NAME & ADDRESS (if different from Controlling Office): Electronic Systems Division Hanscom AFB Bedford, MA 01731	15. SECURITY CLASS. (of this report): Unclassified
	15a. DECLASSIFICATION DOWNGRADING SCHEDULE

16. DISTRIBUTION STATEMENT (of this Report)

Approved for public release; distribution unlimited.

17. DISTRIBUTION STATEMENT (of the abstract entered in Block 20, if different from Report)

18. SUPPLEMENTARY NOTES

None

19. KEY WORDS (Continue on reverse side if necessary and identify by block number)

Ballistic Missile Defense (BMD)
Closely Spaced Object (CSO)
Cramer-Rao bound
detection
simulation
optical targets
estimator

20. ABSTRACT (Continue on reverse side if necessary and identify by block number)

In this report the detection and estimation of closely spaced optical targets are studied using simulation. The observed signal which originates from two point targets may exhibit only one apparent peak when they are located within one detector width. The Akaike information criterion and a maximum likelihood estimator are used to detect and estimate such unresolved targets. For target separation between 3/4 and 1 detector width the detection rate is high, the estimator is unbiased and the estimation variance is close to the Cramer-Rao bound. The performance degrades greatly when the separation becomes smaller. This loss in performance is attributed to the increasing interference between the two targets and the difficulty in providing a "good" initial guess for the estimator.

DD FORM 1 JAN 73 1473 EDITION OF 1 NOV 65 IS OBSOLETE

UNCLASSIFIED

SECURITY CLASSIFICATION OF THIS PAGE (When Data Entered)

207650